PSERC

Consequences of Fault Currents Contributed by Distributed Generation

Intermediate Project Report

Power Systems Engineering Research Center

A National Science Foundation
Industry/University Cooperative Research Center
since 1996

Power Systems Engineering Research Center

Consequences of Fault Currents Contributed by Distributed Generation

Intermediate Report for the Project "New Implications of Power System Fault Current Limits"

N. Nimpitiwan
G. T. Heydt
Arizona State University

PSERC Publication 04-34

November 2004

Information about this project

For information about this project contact:

G. T. Heydt
Regents' Professor
Arizona State University
PO Box 875706
Tempe, AZ 85259-5706
Tel: 480-965-8307
Fax: 480-965-0745
Email: Heydt@asu.edu

Power Systems Engineering Research Center

This is a project report from the Power Systems Engineering Research Center (PSERC). PSERC is a multi-university Center conducting research on challenges facing a restructuring electric power industry and educating the next generation of power engineers. More information about PSERC can be found at the Center's website: http://www.pserc.wisc.edu.

For additional information, contact:

Power Systems Engineering Research Center
Cornell University
428 Phillips Hall
Ithaca, New York 14853
Phone: 607-255-5601
Fax: 607-255-8871

Notice Concerning Copyright Material

Acknowledgements

The Power Systems Engineering Research Center sponsored the research project titled "New Implications of Power System Fault Current Limits." This project is underway at the time of writing (November, 2004). This report is an intermediate report of progress at Arizona State University.

We express our appreciation for the support provided by PSERC's industrial members and by the National Science Foundation under grant NSF EEC-0001880 received under the Industry / University Cooperative Research Center program.

The authors thank all PSERC members for their technical advice on this project. Special thanks go to Dr. R. Thallam and Messrs. J. Blevins and A. B. Cummings of Salt River Project for their technical input. We are also indebted to Professors A. Bose and A. P. S. Meliopoulos of Washington State University and Georgia Tech respectively for their work on this project.

Executive Summary

This report concerns fault currents in systems with distributed generation. The main concept described is that fault current throughout power systems is likely to increase when distributed generation is installed. The nature of the increase is described in some detail, mainly using the Z_{bus} method of calculation. IEEE standards are used to apply correction factors. The requirements of IEEE Standard 1547 are applied as well – this is a standard for distributed generation use.

Fault calculations in power systems are used to determine the interrupting capability of circuit breakers. The calculation of fault current at the system buses is done by applying the system Z_{bus} matrix. The effects of merchant plants, such as Independent Power Producers, are not taken into consideration in the classical fault current calculation. New developments in deregulation have brought new generation sources to the system. The appearance of DGs is a cause of increasing fault currents that has not previously been envisioned. This report presents a modification of the conventional fault current calculation in the case of addition of DGs. Many consequences arise from increasing of the fault currents, for instance the change of coordination of protective devices, nuisance trips, safety degradation, and the requirement to change recloser and protective relay settings. These consequences result in the cost of equipment upgrades not only at the DG sites but also other system sites.

Due to installing new DGs, six main factors that affect the severity of the increase of three phase fault current at each buses are:

- the number and size of DGs
- the operation of the AVR
- the impedance of DGs
- the location of DGs
- the type of DGs
- circuit breaker configuration.

In the report, an index called the average change of fault current or "ACF" is proposed. The ACF can be used to indicate the severity of the change of fault current due to installing new DGs. Chapter 4 proposes the least squares method to approximate the ACF for a given system. By this proposed technique, the pre-fault voltages and the fault current calculation may not be needed in the preliminary design stage. Note that in the preliminary design stage there may be a very large number of calculations, and the ACF concept can speed up the analysis. The only required input of the least squares method is the impedance of a new DG and its location. The advantages of this technique are:

- faster calculation due to the fact that load flow solution and fault calculations are not required
- contribution of the increase of fault current is indicated at each location of 12 kV bus in the primary distribution system. By this concept, each new DG is treated in an equitable way. The ACF concept is offered as a rapid way to assess fault currents when DGs are deployed in any number, anywhere in the system.
- The main disadvantage of the ACF method relates to accuracy. That is, even though the estimator may have been constructed for a large number of sample cases, there is no guarantee that the ACF calculation will be accurate.

Table of Contents

Table of Figures

Table of Tables

Nomenclature

AC	Alternating current
ACF	Average change of fault current
$ACF_{(bus)}$	Bus ACF
AVR	Automatic voltage regulator
CAAA	Clean air act amendments
CB	Electric circuit breaker
CHP	Combined heat and power
CIGRE	International Council on Large Electricity Systems
DC	Direct current
DG	Distributed generation
DG_{imp}	Impedance of distributed generator
DOE	Department of Energy
DR	Distributed resource
E	Pre-fault voltage
EA	Evolutionary algorithm
ECED	Environmentally constrained economic dispatch
ED	Economic dispatch
EIC	Equal incremental cost method
EMI	Electromagnetic interference
EP	Evolutionary programming
EPRI	Electric Power Research Institute
EPS	Electric power system
ES	Evolutionary strategy
E/X	Ratio of system voltage and equivalent reactance
f_j	Function applied in the least squares estimator
F	Relationship matrix
F^+	Pseudoinverse of the relationship matrix
FCL	Fault current limiter
GA	Genetic algorithm
GP	Genetic programming
HGA	Hierarchical genetic algorithm
i	Complex number $\sqrt{-1}$
IC	Current interrupting capability
IPP	Independent power producer
I_{fj}	Fault current at bus j
$I_{f,n}$	Fault current at bus n before installing new DG
$I_{fDG,n}$	Fault current at bus n after installing new DGs
I_p	Injected current at bus p
j	Complex number $\sqrt{-1}$
k	Order of the function applied in the least squares estimator
λ_{qr}	Primitive line impedance from bus q to bus r
m	Number of the bus with DG
MM	Minimum melting time of fuse

MTG	Microturbine generators
MCFC	Molten carbonate fuel cells
n	Number of all historical data
nDG	Number of bus with DG
$nbus$	Total buses in the system
NUG	Non-utility generator
OPF	Optimal power flow
p	Number of the coefficient of the least squares estimator
PAFC	Phosphoric acid fuel cells
PCC	Point of common coupling
PEM	Proton exchange membrane
P_{DG}	Critical power rating of distributed generation
PV	Photovoltaic
q	Number of the historical data (cases)
r	Residual of the least squares estimator
RRRV	Rate of rise recovery voltage
SFCL	Superconductor fault current limiter
SOFC	Solid oxide fuel cell
SS_{Res}	Residual or error sum of squares
SRP	Salt River Project
$t_{\alpha/2,n-p}$	Value from t-distribution
TC	Total clearing time of fuse
UF	Fraction of the total cost paid by utility company
V_i^0	Voltage at bus i before installing DG
V_f	Pre-fault voltage
V_j	Voltage at bus j during fault
w	Coefficient vector
$\hat{w}$	Estimate value of w
X_0	Zero sequence equivalent reactance of the system
X_1	Positive sequence equivalent reactance of the system
X	System reactance
X/R	Ratio of system equivalent reactance to system equivalent resistance
y	Output vector of the least square estimation technique
Z_{bus}	Bus impedance matrix
Z_{bus}^+	Positive sequence bus impedance matrix
Z_{bus}^-	Negative sequence bus impedance matrix
Z_{bus}^0	Zero sequence bus impedance matrix
$z_{gen}^{(b)}$	Generator transient impedance
$z_{DG,\lambda}$	Transient impedance of DG at bus λ case b
Z_{orig}	Bus impedance matrix of original system
z_f	Fault impedance
$Z_{ij,orig}$	Diagonal element of bus impedance matrix of the system before installing new DG

$Z_{ij,new}$	Diagonal element of bus impedance matrix of the system after installing new DG
$\Delta \lvert I_f \rvert$	Change of fault current due to installing new DGs
$\Delta \lvert V \rvert$	Change in voltage
σ_r^2	Variance of residual
$\sigma_r^{\ 2}$	Estimation of variance of residual
$\{\Omega\}$	Off line analyzed cases

1. Introduction

1.1 Motivation

Deregulation, utility restructuring, technology evolution, environmental policies and increasing electric demand are stimuli for deploying new distributed generation (DG). According to the US Department of Energy (DOE), DG is defined as [5] "the modular electric generation or storage located near the point of use. Distributed generation systems include biomass-based generators, combustion turbines, thermal solar power and photovoltaic systems, fuel cells, wind turbines, microturbines, engines/generator sets and storage and control technologies. Distributed resources can either be grid connected or independent of the grid. Those connected to the grid are typically interfaced at the distribution system". According to the IEEE Standard 1547-2003, DG is defined as "Electric generation facilities connected to an area Electric Power System (EPS) operator through a Point of Common Coupling (PCC); a subset of Distributed Resource (DR)" [6]. Reduction of investment in transmission and distribution system upgrades and fast installation are the major benefits to the power utilities. Many applications, such as upgrading the reliability of the power supply, peak shaving, grid support and combined heat and power (CHP), are the major benefits to distributed generation owners.

However, the appearance of co-generation, DG, and unconventional generation may result in unwanted (and often unexpected) consequences. This report focuses on one such unwanted consequence: increased fault current. In this report focus is given to operation during faulted conditions. Circuit breaker capability and configuration of protective relays that were previously designed for the system without DGs may not safely manage faults. There may be some operating and planning conditions that are imposed by the fault current interrupting capability of the existing circuit breakers and the protective relay configurations. These situations can result in the safety degradation of the electric power system. At present, there is a very low penetration of DG in the United States (about 18 % of the total installed generation capacity is DG according to [21]). However, many indicators imply that DG penetration is increasing. The cited fault current concerns are expected to occur at higher levels of DG penetration. Also, *locally* DG penetration could be high in some circumstances. The identification and alleviation of degraded operation of power systems during fault conditions is the main objective of this work.

Assessment of the ability of power systems to manage the increase of fault currents due to DGs should be investigated. Fault currents in power systems determine the ratings of the circuit interruption devices and the settings of power system protective relays. Once the circuit breakers are in place and relay settings have been implemented, there may be some operating and planning implications imposed by the changing fault current. Fault analysis should be done prior to the installation of a new DG. A method should be developed to redesign a protection system and associated circuit interruptions. The objective is to minimize the need to replace (upgrade) the existing equipment and/or assign the costs of upgrading to the customers that have installed DG. In some cases, entirely new protective relay settings and upgraded circuit breakers may be needed. This is a complicated issue which depends on the type of the customer, the size and the type of the DG equipment, and the operating intention of the DG system.

Who should pay the extra cost of installing new DG, such as upgrade protection system and maintenance, needs to be addressed. All approaches to allocate the responsibility and the cost of these changes should be on the basis of simple and fair market for every customer and utility. The identification of what is fair and what is simple has not been done for the case of

fault currents due to added DGs. Possible alternatives are:

- The owner of the DG pays for all system changes and upgrades.
- The owner of the DG shares the cost of the system changes and upgrades with the electric utility company on the basis of the system reliability prior to the installation of the DG. That is, the DG owner has installed the DG because of reliability issues due to the utility company, and therefore the utility company should share the cost of the upgrades needed. Under such a policy, if the primary distribution system reliability fell below a certain level, the cost of DG upgrades would be shared by the DG owner and the utility company – by an agreed formula.
- Special tariffs for customers with DGs should be approved to create a fund for the payment of required system upgrades.

These issues are needed to guarantee safety and reliability of the system which should be covered by the owner of the DG.

1.2 Objectives

The main objective of this research is to establish an algorithm for the identification of optimized operating limits imposed by system fault current interruption capability. Also, identify the locations and techniques which improve the fault interruption capability where the protection system needs to be upgraded. For this purpose, the technical approaches for these objectives are:

- Modeling of different types of DG
- AC fault analysis
- The identification of operating conditions and hardware
- Modification of standard Optimal Power Flow (OPF) algorithms to accommodate fault current limitation.

1.3 Literature review: distributed generation

In this section and the subsequent two sections, a brief overview of pertinent literature is given. The overview is organized into three sections, and ten subsections: (in Section 1.3)

- Distributed generation
- Non-utility generators
- Installing DG
- Impact of DGs on fault current and system protection.

(in Section 1.4)

- The IEEE Standard 1547
- The IEEE Standard C37.04-1999.

(in Section 1.5)

- Optimal power flow
- Stability constrained OPF
- Environmentally constrained economic dispatch
- Fault current limiters.

Distributed generation

The size and type of DGs various over a wide range and definitions and commonly encountered DGs depends on factors such as:

- DOE considers DG range from less than a kW to tens of MW [5]

- The Electric Power Research Institute (EPRI) considers DGs from a few kW to 50 MW or energy storage devices sited near customer loads [20]
- Gas Research Institute considers DGs between 25 kW to 25 MW [23]
- The International Council on Large Electricity Systems (CIGRE) considers DGs as a generation unit that is not centrally planned, not centrally dispatched and smaller than 100 MW [24].

Since the 1990s, reciprocating engines and gas turbines have been rapidly placed into service. Perhaps this deployment is a result of problems in dealing with transmission issues, and problems in siting conventional generation – but, for whatever reason, protection engineers as well as transmission and distribution engineers have to increasingly deal with problems related to the added DG in the power systems. Reference [5] indicates that the standby DG application continues to grow at approximately 7% per year. Other DG applications, base load and peak load, are growing faster at 11% and 17%, respectively. The market size of these three sectors is about 5 GW in 2004. Figure 1.1 shows the applications for reciprocating engines and gas turbines (less than 20 MW).

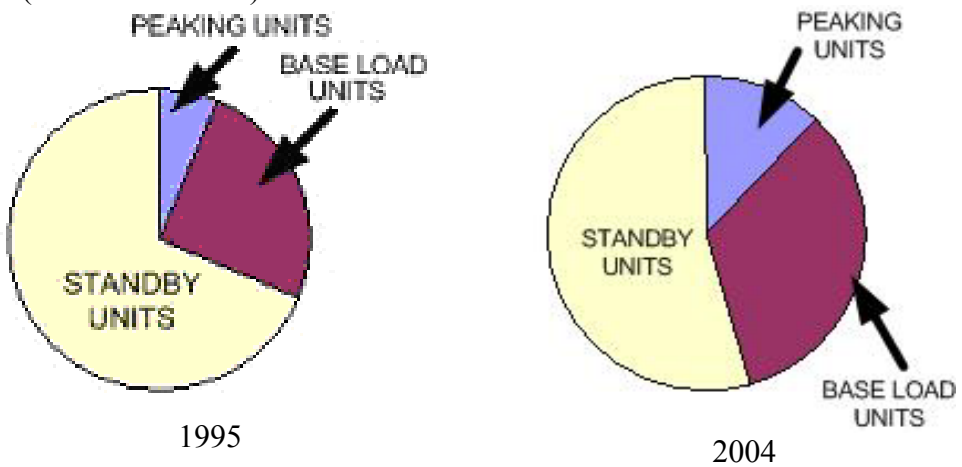

Figure 1.1 Reciprocating engines and gas turbines less than 20 MW (data from [5]) in 1995 and 2004

The emergence of small and medium size DG arises from two major necessities: inadequacy of efficient power production (both economy and environment friendly) and requirement of high reliability from industrial or commercial customers with a very high value product. Table 1.1 shows approximate data for the cost of DGs per kW [19].

Distributed generation can appear in different forms, both renewable and nonrenewable. Renewable technologies include fuel cells, wind turbine, solar cell, and geothermal. Nonrenewable technologies include combined cycles, cogeneration, combustion turbine and microturbines. References [21, 22] made a brief discussion on DG technologies which are available in the market.

Table 1.1 Approximate price of DG per kilowatt [19, 28]

Technology	Size Range (kW)	Approximate Cost ($/kW)
Diesel engine	20 - 10,000	125 - 300
Turbine generator	500 - 25,000	450 - 870
Wind turbine	10 - 1,000	~ 1,000
Microturbine	30 - 200	350 - 750
Fuel cell	50 - 2,000	1,500 - 3,000
Photovoltaic	<1 - 100	~ 3,000

The theoretical basis of a fuel cell was explored by Sir William Grove in 1839 [22]. Grove discovered that water can be decomposed into hydrogen and oxygen by applying electric current, a process called "electrolysis". As shown in Figure 1.2, the basic operation of fuel cell is the reverse of electrolysis – the hydrogen and oxygen recombine and electric current is the product of this reaction. There are many types of fuel cells which can be applied to industrial applications, especially CHP. Table 1.2 provides brief information on different types of fuel cells.

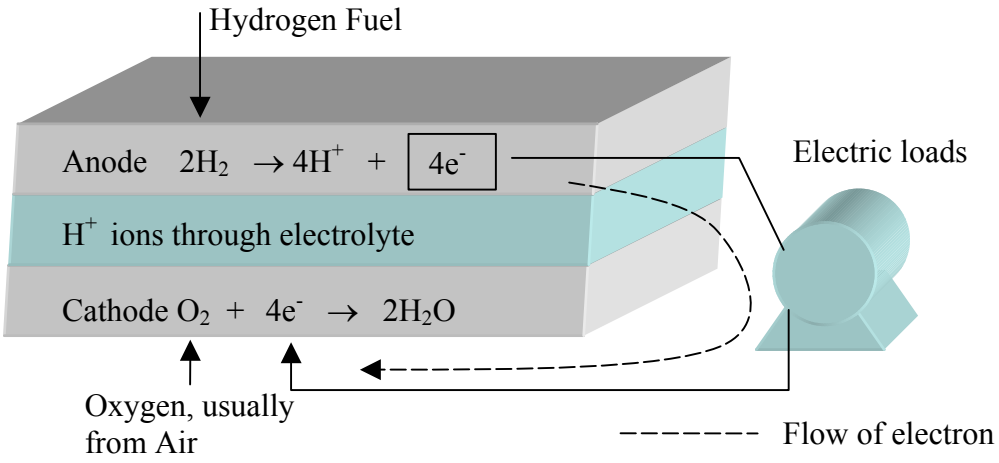

Figure 1.2 Electrode reactions and charges flow for an acid electrolyte fuel cell [25]

A problem with electrolysis based technologies is inefficiency, mainly due to resistive heating (due to passage of current through water). There are other processes that have been suggested to produce hydrogen, but all have efficiency concerns.

Microturbine generators (MTGs) were originally developed for military to produce electricity. Normally, an MTG produces high frequency AC. For connecting the high frequency AC output to the grid system, it must be rectified to DC and then inverted to the power frequency. The major advantages of MTG are: ease of installation, simple siting/licensing, and lower capital requirements [22]. Disadvantages relate to the cost of the power electronics needed. In order to obtain high efficiency units, the waste heat from MTGs must be utilized.

A photovoltaic (PV) system generates electricity by the direct conversion of the light en-

ergy into electricity. The key component of a PV is a solar cell which requires sophisticated semiconductor processing techniques to be manufactured. PV operation can be separated into two parts: conversion of solar energy to electric energy and grid connection system. Simulation of both parts is discussed in [27] using PSpice.

Table 1.2 Data for different type of fuel cells [26]

Fuel Cell Type	Electrolyte	Charge Carrier	Operating Temperature	Fuel	Electric Efficiency (system)	Power Range/ Application
Proton Exchange Membrane (PEM)	Solid Polymer	H^+	50-100 °C	Pure H_2	35-45%	5-250 kW, Automotive or small CHP
Phosphoric acid (PAFC)	Phosphoric acid	H^+	~ 220 °C	Pure H_2	40%	200 kW , CHP
Molten carbonate FC (MCFC)	Lithium and potassium carbonate	CO_3^{2-}	~650 °C	H_2, CO, CH_4, other hydrocarbon	>50%	200 kW - MW, CHP
Solid oxide FC (SOFC)	Solid Oxide electrolyte	O^{2-}	~ 1000 °C	H_2, CO, CH_4, other hydrocarbon	>50%	2 kW - MW, CHP

Non-utility generators

Increasing of non-utility generators (NUGs) rapidly increases consideration of effects of distributed generations to the grid. Statistics show that by the end of the decade, the proportion of total capacity and DG capacity will grow to 20 percent or approximately from 40 GW to more than 150 GW [7].

Installing DG

Installing DG at a customer site enhances certain aspects of the power quality of the owners significantly by mitigating the voltage sag during a fault. Most faults on a power system are temporary, like arcing from overhead line to ground or between phase conductors. These temporary faults on a distribution system should be detected and cleared by protection relays and reclosers. During the period of the fault, the voltage in the distribution system drops. This phenomenon is called “voltage sag”. The magnitude of the sag is dependent on the line impedance from substation to the fault location. Locally installed distributed generation at customer sites can provide voltage support during faults in the utility transmission system and improve the voltage sag performance. Moreover, DG improves the owner reliability markedly as a typical back up generator can be started up within 2 minutes.

Although there are many advantages of installing DGs, a few operating conflicts cannot be ignored. If there is a high penetration of DGs, the conventional utility supply may not be able to serve the load if the DGs drop off-line [10]. Installing a small or medium DG may not have a significant impact on the power quality indices at the feeder-level. The main reason for this ob-

servation is that IEEE Standard 1547 requires that the load be disconnected from the supply feeder after a specified period of time (a rather short time, measured in cycles). The DG, after the cited disconnection, will have no impact on the supply feeder. The DG has a local impact. That is, the local load may be served properly, but others on the common feeder will not experience improvement in voltage regulation.

Installation of DGs has been discussed in many research papers, such as those dealing with the reliability of the distribution system, coordination of protective devices, ferroresonance, frequency control, and consequences of increased fault current [8]-[10], [23].

Impact of DGs on fault current and system protection

Protection system planning is an indispensable part of an electric power system design. Analysis of fault level, pre-fault condition, and post-fault condition are required for the selection of interruption devices, protective relays, and their coordination. Systems must be able to withstand a certain limit of faults that also affects reliability indices. Many classical references are found on this topic, such as [1] - [4]. This research relates to a new aspect of fault analysis of power systems: the appearance of DG, perhaps at high levels of penetration, and the effect of DG on fault currents.

In general, addition of generation capacity causes fault currents to increase. The severity of increasing fault current in the system depends on many factors which are penetration level, impedance of DG, the use of Automatic Voltage Regulator (AVR), power system configuration, and the location of DG – approximately in that order. This is a simple consequence of the reduction of the Thevenin equivalent impedance seen at system buses when generation is added to the system. The theory and details of the fault current analysis are discussed in Chapter 2. The consequences of increased fault current from proliferation of distributed generation are discussed as follows:

- *Change in coordination of protective devices:* Figure 1.3 shows a sample distribution system. This system is a primary distribution system that is offered as an example of a distribution system with three DGs. The system is purely radial, three-phase, 4160 V, and served from a 69 kV subtransmission system at a substation. In the depicted configuration, the protection system may lose coordination upon installation of a DG. This point is illustrated as follows: before installing distributed generation DG1, if a fault occurs at point 1, fuse A should operate before fuse B. This is due to the upstream fault on the sub-feeder. When DG1 is included on sub-feeder, the fault current flows from DG1 to fault point 1 and fuse B might open before fuse A if the difference between I_{FA} and I_{FB} is less than the margin shown in Figure 1.4. The difference between I_{FA} and I_{FB} is proportional to characteristics of DG1. Thus, these fuses lose coordination in the case of installed DG1 [8]-[9].

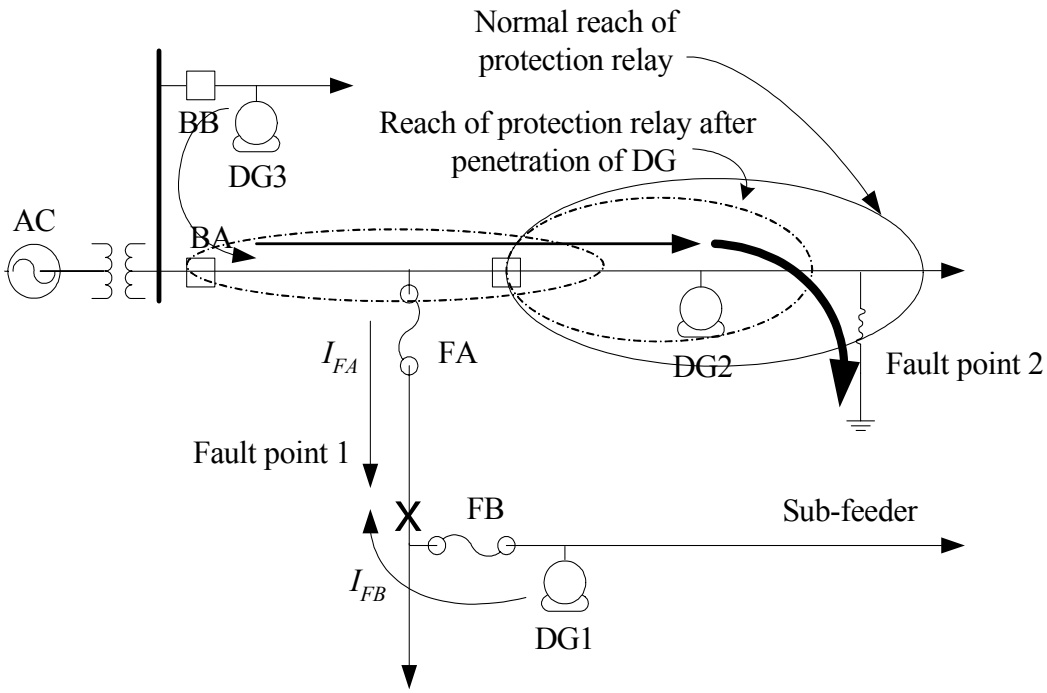

Figure 1.3 The reach of a protective relay for a small sample distribution system with DGs, from Nimpitiwan [32]

- *Nuisance trip:* The increasing of fault current in the grid changes the way that protection system manages faults (relay settings, reclosers, interrupting capability of circuit breakers and fuses). Figure 1.3 shows a relatively large DG3 installed near the substation. In case a fault occurs on feeders other than where DG3 is located, breaker BB might also trip due to the fault current flowing from DG3 to the fault point. The solution for this problem is to implement a directional relay instead of an overcurrent relay. This is a total reconfiguration of the protective relaying.

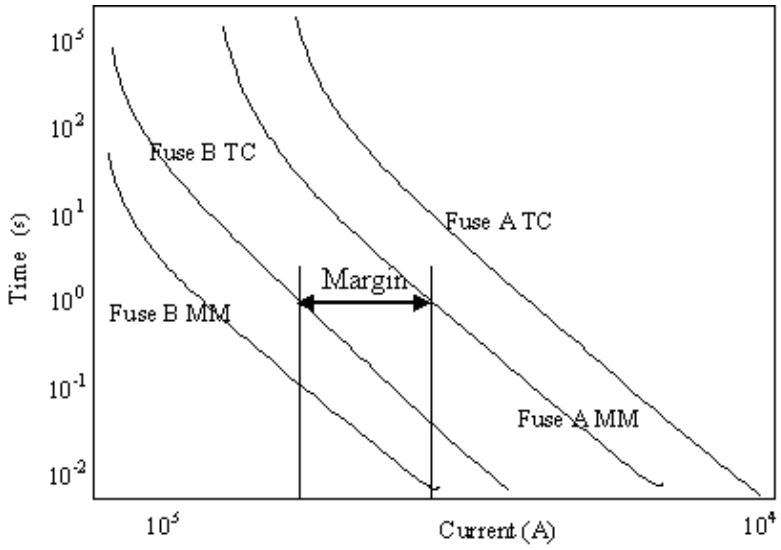

MM: Minimum melting TC: Total clearing

Figure 1.4 Time-current characteristic of the fuse in the sample system of Figure 1.3 from Nimpitiwan [32]

- *Recloser settings:* A DG on the feeder normally requires that the utility to readjust their recloser settings. Normally, a DG must detect the fault and disconnect from the system within the recloser interval and leave some duration for the fault to clear. Failure to follow this step might cause a persistent fault rather than a temporary one. Reference [11] recommends a recloser interval of 1 second or more. The IEEE Standard 1547 [6] requires a much shorter time for recloser.
- *Safety:* Safety degradation from the failure of protection system may occur because a new DG increases the fault current. If the fault current is higher than the previous level, that is higher than the interrupting capability of circuit breaker, the fault current might persist and cause damage to personnel and equipment.
- *Changing the reach of protective relays:* A DG may reduce the reach of power system protective relaying under certain circumstances. Consider a resistive fault occurring at fault point 2 during the peak load as shown in Figure 1.3. The presence of DG2 in between the fault point might cause a lower fault current to be seen by the protective relay. The DG effectively reduces the reach (i.e., zone) of the relay. This increases the risk of high resistive faults to go undetected. In such a case, backup protection may operate to interrupt a fault.

1.4 IEEE Standards

In this section, the IEEE Standards 1547 [6] and C37.04-1999 [29] are discussed. Standard 1547 relates to DGs and C37.04 relates to fault current interruptions.

The IEEE Standard 1547

This standard provides the specifications and requirements for interconnection of DR with area EPS. According to this standard, DR is defined as sources of electric power including both generators and energy storage technologies. DG is the electric generation facility which is a subset of DR. The requirements for interconnection of DR under normal conditions specified in

the IEEE Standard 1547 are:

- the voltage regulation of the system after installing DG is ± 5 % on a 120 volt base at the service entrance (billing meter) [36]
- the DR unit should not cause the voltage fluctuation at the PCC higher than ± 5 % of the prevailing voltage level of the local EPS
- the network equipment loading and IC of protection equipment, such as fuse and CB should not be exceeded
- the grounding of the DR should not cause overvoltages that exceed the rating of the equipment in local EPS.

The requirements for interconnection of DR under abnormal conditions are:

- the DR unit should not energize to the area EPS when the area EPS is out of service
- the DR unit should not cause the misoperation of the interconnection system due to Electromagnetic Interference (EMI)
- the interconnection system should be able to withstand the voltage and current surges
- the DR unit should cease to energize the area EPS within the specific clearing time due to abnormal voltage and frequency
- the DR unit should not cause power quality problems higher than specified tolerable limits, such as DG harmonic current injection, flicker and resulting harmonic voltages.

In case the system frequency is lower than 57 Hz, the DR unit should cease to energize to the area EPS within 16 ms. When a fault is detected, the DGs must be disconnected from the electric utility company supply and the DG should pick up the local load. The disconnection is needed because: (1) a fault near to the DG in the supply system must be interrupted and (2) the local DG can not support the power demands of the distribution system (apart from the local load). The disconnection of the DG from the network must occur rapidly. Table 1.3 shows the IEEE 1547 requirement [6] for disconnection times.

Table 1.3 Required clearing times for DGs higher than 30 kW, from IEEE 1547 [6]

Voltage Range	Clearing time (s)
$V < 50$	0.16
$50 \le V < 0.88$	2.00
$110 < V < 120$	1.00
$V \ge 120$	0.16

Note that the foregoing remarks related to the cost of added equipment and upgrades due to fault currents are separate from the issues related to commonality of technical conditions at DG sites. Most utilities utilize a common set of rules to interconnect the DG to power system, for example:

- Exchange the project information between utility and customer
- Technical analysis by the utility to evaluate the impact of DGs
- Inspection of interconnection and protective equipment by the utility.

These issues are needed to guarantee safety and reliability of the system which should be covered by the owner of the DG.

The IEEE Standard C37.04-1999

The requirement of sizing the current interrupting capability (IC) of circuit breakers (CBs) is discussed in the IEEE Standard C37.04-1999 [29], "IEEE application guide for AC high voltage circuit breakers rated at symmetrical current basis". In general, a three phase to ground fault imposes the most severe duty on a CB. However, a single phase to ground may produce a higher fault current than a three phase fault. This condition occurs when the equivalent zero sequence at the point of fault is lower than the positive sequence reactance. Two methods for calculating system short circuit current are proposed in [30], the simplified *E/X* method and the *E/X* method with adjustment for AC and DC decrements.

The simplified method for calculating system short circuit current requires only a simple E/X_1 calculation for three phase faults or $3E/(2X_1+X_0)$ for single phase to ground faults, where E is the highest system pre-fault voltage, X_1 and X_0 are the positive/negative and zero equivalent reactance of the system at the circuit breaker location. For higher accuracy of symmetrical fault current calculations, the impedance of rotating equipment should be multiplied by the impedance multiplier factors given in [30]. Note that the *E/X* simplified method is utilized without considering the system resistance, *R*. For this reason, this method is applicable only when the *E/X* of the system does not exceed 80 percent of the symmetrical interrupting capacity of the breaker [30]. The rated IC of circuit breaker can be selected from the preferred rating schedules in [31].

For higher accuracy than the previous method, the *E/X* method with adjustment for AC and DC decrements should be used. This method takes the decrement of the AC and DC components of the fault currents into account by applying factors to *E/X* calculation. The multiplying factor depends on the point where the short circuit occurs and the system *X*/R ratio as seen from the considering point. After calculating the *X/R* ratio, the multiplying factor is given in Figures 1.5 and 1.6. These figures are taken directly from [31] and reproduced here for ease in reading. Note that the system reactance (*X*) is calculated by completely disregarding the system resistance, *R*, and vice versa. The resulting product of the system *E/X* and the multiplying factor must not exceed the symmetrical IC of the circuit breaker under consideration. Examples of choosing the IC of a circuit breaker are given in [30] and [32].

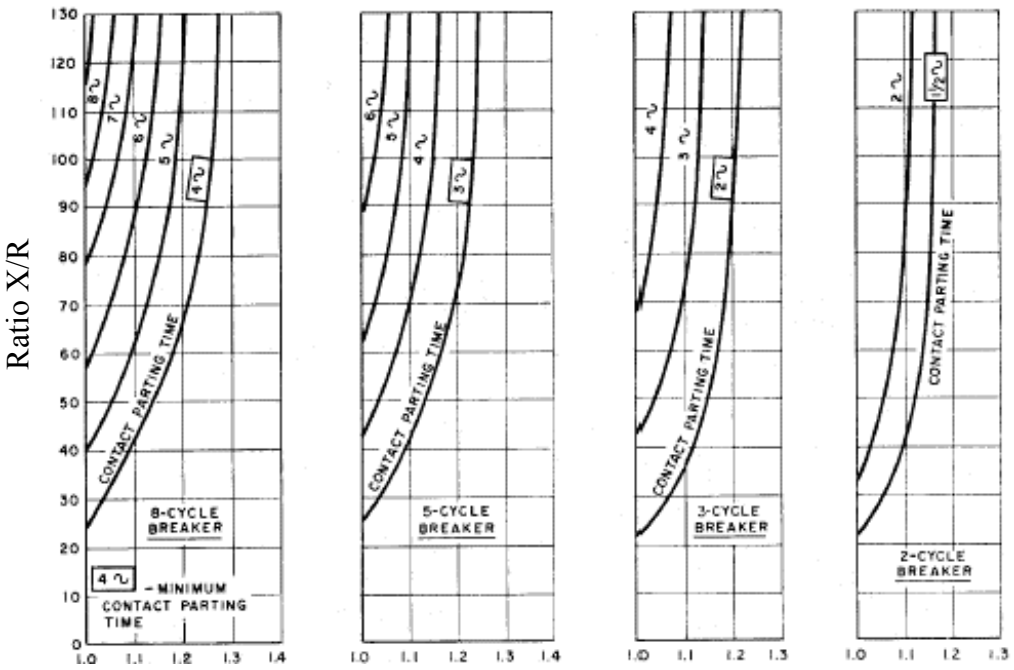

Figure 1.5 Three phase fault multiplying factors [31]

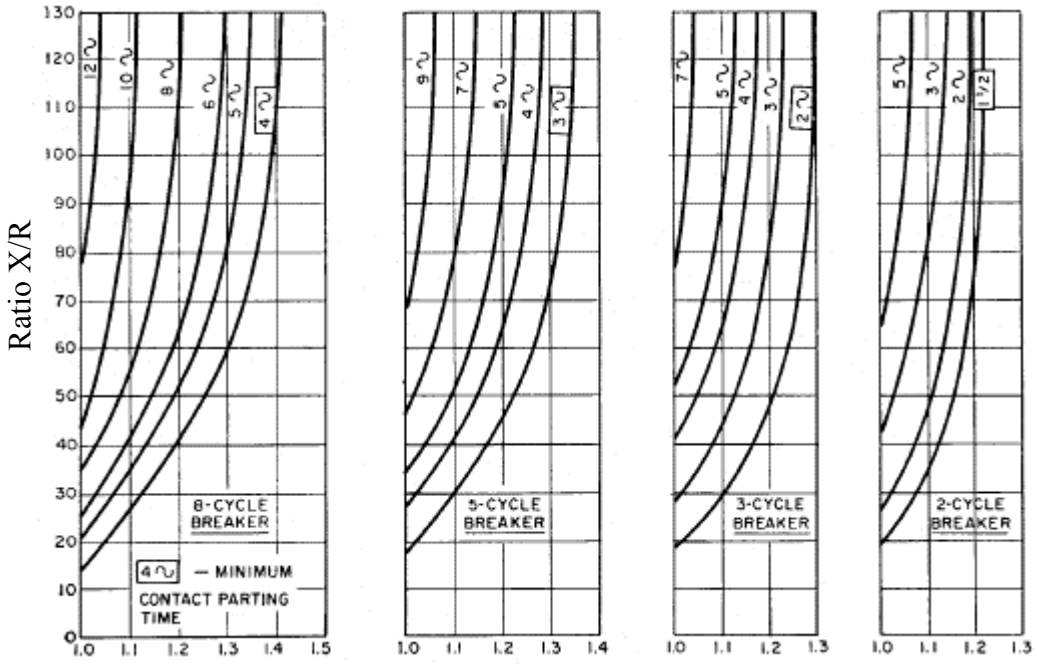

Figure 1.6 Line-to-ground fault multiplying factors [31]

1.5 Literature review: systems and hardware

In this section, selected aspects of operating limits and hardware to accommodate fault current are reviewed.

Optimal power flow

Optimal power flow (OPF) studies have been discussed since its introduction in the early 1960s [39]. References [51, 52] have an excellent literature survey in this topic. Historically, the economic dispatch (ED) by the Equal Incremental Cost Method (EIC) was the precursor of OPF. The EIC method is a type of OPF, and the objectives is to minimize fuel cost (i.e., the EIC method minimizes fuel cost; other OPF methods may have other objectives and constraints as well. An example of OPF that considers reactive power is the Dommel-Tinney method [63].

Classical optimization methods in general can be classified into two groups: direct search methods and gradient-based methods [46]. In direct search methods, the objective function and the constraints are used to guide the search strategy. Since the direct search methods do not require the derivative information, they are often slow and require many function evaluations for convergence. In the gradient based methods, the first (and possibly the second) derivative of the objective and the constraints guide the search strategy. Usually, the gradient based methods converge to the optimal solution faster than the direct search methods. However, gradient based methods may not be capable of solving the non-differentiable or discrete problems.

The majority of the classical techniques to solve non-linear programming problems discussed in the OPF literatures are:

- lambda iteration method or also called EIC
- gradient method
- Newton's method
- linear programming method
- interior point method.

References [1, 2, 35, 40, 41] have introductions to these topics. Typical objectives of the OPF are minimization of fuel cost, losses and added VARs while maintaining the system constraints. The control variables of the OPF are generator bus voltages, transformer and phase shifter settings and real power at the generator bus. The constraints of the OPF may include generator bus voltages, line flows, transformer capacities and phase angle regulator settings, security constraints, stability constraints, environmental constraints and reliability constraints.

References [46, 49, 50] discuss some difficulties of using the classical techniques to solve the optimization problems, such as:

- The convergence to an optimal solution depends on the chosen initial condition. Inappropriate initial condition makes search direction converge into a local optimal solution.
- The classical techniques are inefficient in handling problem with discrete variables.

The following section illustrates the performance and applicability of the OPF with various constraints.

Stability constrained OPF

Stability is an important constraint in power system operation. The cost of losing synchronism through a transient instability is high in power systems. A large number of transient stability studies may be needed to avoid this problem. Transient stability may be considered as an additional constraint to the normal OPF with voltage and thermal constraints. In the normal OPF, it is well-understood that the voltage and thermal constraints can be modeled by a set of algebraic equations. However, the stability constrained OPF contains a set of both differential

and algebraic equations. The dependence on time is an added level of complexity.

Gan and Thomas in [42] propose a technique to solve this problem by converting the differential- algebraic equations to numerically equivalent algebraic equations. The stability constraints are expressed by the generator rotor angle and the swing equations. LP method with relaxation technique is implemented to solve the OPF problem.

Environmental constraints

According to the requirements of the Clean Air Act Amendments (CAAA), the electric utility industry has to limit the emission of SO_2 to 8.9 million tons per year and multiple NO_x to 2 million tons per year [43, 44]. The emission rate of each unit can be expressed as a quadratic function of generation active power output (MW) and heat rate (MBtu/h). Emission control can be included in the conventional ED problem by adding the environmental cost to the normal dispatch.

Several authors [45-48] apply Evolutionary Algorithm (EAs) to solve the ED problem. The EAs are computer-based problem solving systems. These methods mathematically replicate the mechanisms of natural evolution as the key elements in their design and implementation. Four different EAs are genetic algorithms (GAs), evolutionary strategy (ES), evolutionary programming (EP) and genetic programming (GP). Deb in [48] describes the theory of the multi-objective optimization by applying the EA.

Wong and Yuryevich in [45] apply the EP technique to solve the Environmentally Constrained Economic Dispatch (ECED) problem. The EP technique is based on the mechanics of natural selection. Basically, EP searches for the optimal solution by evolving population candidate solutions over a number of generations or iterations [45]. A new population or *individual* is produced from an existing population through a process called "mutation". Individuals in each generation and the mutate population compete with each other through a competition scheme. The winning individuals from the competition scheme form a next generation. The process of evolution may be terminated by two stopping criteria: stop after a specified number of iterations or stop when there is no significant change in the best solution.

Yalcinoz and Altun in [47] and Ma, El-Keib and Smith in [48] propose a solution for ECED problem using modified genetic algorithm. The objective function consists of three terms which are the production cost, emission functions of SO_2 and NO_x. The authors conclude that the proposed GA algorithm is appropriate to be applied to solve the ECED problem.

The foregoing advanced intelligent based algorithms are reasonably well documented in the literature, but there are no known actual applications in operational power system dispatch.

Fault current limiters

A fault current limiter (FCL) is a variable impedance device connected in series with a circuit breaker to limit the current under fault conditions. Ideally, the FCL should have very low impedance under the normal operating condition and high impedance under fault condition. The impedance during fault condition should limit the fault current to be below the interruption capability of near by CBs.

The idea of an FCL has been proposed in 1970s. Various types of FCL have been developed based on alternative techniques, such as superconductivity phenomena, power electronics, positive temperature coefficient and the technique of arc control.

Karady in [62] proposed a FCL with series compensation. The author provides the principle of operation and mathematical analysis in the paper. Basically, a non-superconducting FCL is a series capacitor inserted in a line and paralleled with a controlled reactor. The effective impedance of the non-superconducting FCL can be adjusted by the firing angle of the controlled

reactor. During normal operation, the series capacitor provides the series line compensation which helps to increase the maximum power transfer to the line. During fault condition, the controlled reactor operates such that the effective impedance of the non-superconducting FCL is high enough to limit the fault current.

A superconductor fault current limiter (SFCL) was first developed in 1980s. The resistance of superconductor materials changes automatically from zero to high value when current surpasses a certain level. Superconductor material can be classified as two types: low temperature superconductor (LTS) and high temperature superconductor (HTS). LTS has been first discovered in 1983 [53]. However, an FCL based on LTS has never entered the market due to the high cooling cost. The FCL based on HTS was discovered in 1987. HTS can be operated at higher temperatures and needs less refrigeration and therefore less cost. The operating principle of superconductor based FCL can be found in [53, 54, 55, 56].

References [57, 58] investigate the influence of the superconductor based FCL on a simple radial network as illustrated system. Voltage-current characteristics of the superconducting FCL are represented by temperature and current relation. Results of study show that installing superconducting FCLs in power systems has significant increase of the system stability. The SFCL enhances the power system stability by suppressing the excessive kinetic energy of generators. However, the illustrated system is a simple power system; the conclusion might not applicable to the larger mesh power system.

Honggesombut, Mitani and Tsuji in [59] propose a combined method of hierarchical genetic algorithm (HGA) and micro genetic algorithm (micro-GA) to simultaneously determine the optimal location and the smallest SFCL capacity. In problem of assigning the suitable location and the smallest required capacity of SFCL, the search space is large. For this reason, the authors apply the combined HCA and micro GA to improve the efficiency and the searching speed. The proposed technique is applied to a small mesh illustrated system. Results of calculation, optimal location and the smallest SFCL are obtained simultaneously.

Ye, Lin and Juengst in [60] discuss the application of SFCL in power systems. The authors give a theoretical analysis of enhancing power system transient stability. The authors also discuss the mitigation of voltage sags from applying a SFCL in two radial networks connected via SFCL. In such a system, voltage sags are mitigated due to the increasing of fault impedance from the result of the SFCL.

Calixte, Yokomizu, Shimizu, Matsumura and Fujita in [61] present the application of the inductive FCL to a 275 kV system. The effect of inductive FCL on the interrupting conditions imposed on a CB was discussed. The inductive FCL can be used to reduce the fault current. However, the rate of rise recovery voltage (RRRV), which depends highly on the stray capacitance of the FCL, needs to be considered carefully. The lower value of stray capacitance of the FCL limiting coil may lead to an increase in the RRRV and failure interruption.

2. The Theory of Fault Analysis

2.1 The analysis of power system faults

Standard fault analysis techniques have been well studied for many years. This chapter discusses a new topic in fault current analysis, namely the calculation of increasing of fault current due to the installation of new DGs in various scenarios. In order to calculate the fault current at a system bus, a simple Thevenin model is used for the power system. That is, the system is modeled as a voltage behind a system impedance. The system impedance is the Thevenin impedance "seen" at the bus that experiences the fault. The Thevenin voltage is the prefault bus voltage. The Thevenin impedance is simply the *j, j* entry of Z_{bus}, the bus impedance matrix referenced to the system swing bus where *j* is the faulted bus. The Z_{bus} matrix models the entire network (i.e., the transmission network, the subtransmission network, the primary distribution network, and any generators that appear in the system). Generators are modeled as a transient reactance. For example, Figure 2.1 shows the configuration of an unfaulted distribution system and a generator installed at bus *k*. Let the system without the generator at bus *k* be modeled as Z_{orig}. After the addition of the generator at bus *k*, a new bus, bus *p,* is added to the system. These remarks apply to three phase balanced faults. Unbalanced faults can be analyzed through the use of symmetrical components and the corresponding use of Z^{+}_{bus} , Z^{-}_{bus} , and Z^{0}_{bus} .

2.2 Modification of traditional algorithms of fault current calculation

Fault analysis by means of an impedance matrix can be applied to evaluate the incremental fault current due to new generator. Positive sequence models are often adequate for balanced short circuit studies which determine the fault response of a DG [12].

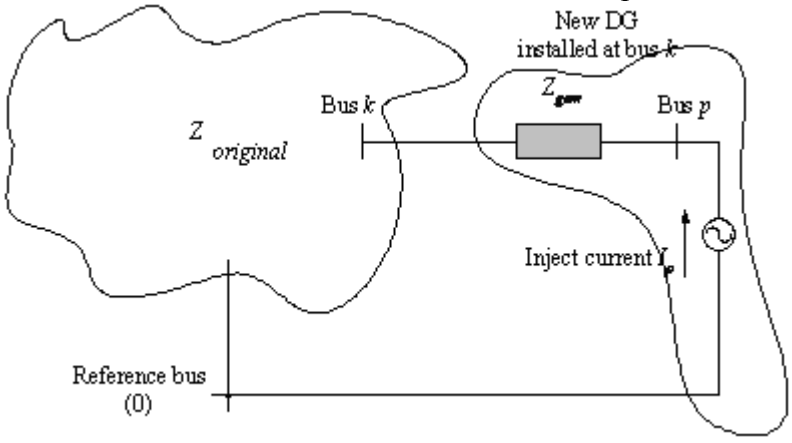

Figure 2.1 New DG added to bus *k* through its internal impedance creating a new bus *p*, from Nimpitiwan [32]

As an example of how a new DG impacts fault response, consider a new DG bus (see Figure 2.1), *p*, of the system connected to an existing bus *k* through the impedance z_{gen}. For the case that the new DG bus is a synchronous generator, the impedance is simply $j\,x'$. The current from the DG injected to the system results in a change of voltage at every bus. The relationship between the new voltages, the injected current I_p, and the off-diagonal elements of bus impedance matrix is given as,

$$V_1 = V_1^0 + I_p Z_{1k}$$
$$V_2 = V_2^0 + I_p Z_{2k}$$
$$\ldots.$$
$$V_k = V_k^0 + I_p Z_{kk}$$
$$V_p = V_k^0 + I_p (Z_{kk} + Z_{gen}),$$

where V_i is the voltage after installing the DG, V_i^0 is the voltage at bus i before installing the DG and Z_{gen} is the impedance of synchronous generator.

In these expressions, the notation Z_{ij} is used to denote the elements of the bus impedance matrix referenced to ground. This matrix, Z_{bus}, includes generators represented as ground ties which are the transient reactances of those generators (for the case of usual synchronous machines). All other ground ties (e.g., capacitors) are modeled in Z_{bus} as well. All the usual faulted power system assumptions are made in constructing Z_{bus} [1]. All equipment (e.g., capacitors, lines) are considered to be in service as a "worst case." the system model equations can be written in matrix form as,

$$\begin{bmatrix} V_1 \\ V_2 \\ \ldots \\ V_n \\ \hline V_P \end{bmatrix} = \left[\begin{array}{ccc|c} & & & Z_{1k} \\ & Z_{orig} & & Z_{2k} \\ & & & \ldots \\ & & & Z_{Nk} \\ \hline Z_{k1} & Z_{k2} & \ldots\ Z_{kN} & Z_{kk} + Z_{gen} \end{array}\right] \begin{bmatrix} I_1 \\ I_2 \\ \ldots \\ I_N \\ \hline I_P \end{bmatrix}$$

or,

$$\left[\frac{V_{orig}}{V_P}\right] = \left[\begin{array}{c|c} Z_{orig} & col_k(Z_{orig}) \\ \hline row_k(Z_{orig}) & Z_{kk} + Z_{gen} \end{array}\right] \left[\frac{I_{orig}}{I_P}\right], \quad (2.1)$$

where N is the row and column dimensions of the original bus impedance matrix, Z_{orig} is the original impedance matrix before installing the generator, Z_{gen} is the transient impedance of the added generator, k is the bus where the generator is installed, p is newly added bus to the system.

The model of the added generation used above is the conventional model of a synchronous generator. Not all DGs are conventional synchronous generators. Many DGs are energy sources that produce DC which is used as the input to an inverter which ultimately interfaces with the AC system. The controls of that inverter determine how the inverter is 'seen' by the network. In many cases, the inverter plus its controls appear as a voltage source and reactance as shown in Figure 2.2. For some inverters, a constant current or constant power control may be used. The constant current model shall be considered below after dealing with the model shown in Figure 2.2. The full treatment of inverter based DGs may not be as easy as these remarks and procedures imply: DG controls are not standardized and control modeling is problematic. For the discussion below, these difficulties are ignored (or relegated to "future work").

Applying the Kron's reduction formula [4] to (2.1), each element of the new bus impedance matrix is

$$Z_{ij,new} = Z_{ij,orig} - \frac{Z_{ik,orig} Z_{kj,orig}}{Z_{kk,orig} + Z_{gen}}. \quad (2.2)$$

Equation (2.2) gives a new bus impedance matrix model for the system with a DG. If there is a fault occurs at bus *j,* as shown in Figure 2.2, the 'injected current' at bus *j* is $-I_j$ (i.e., this is the fault current). From the definition of the bus impedance matrix,

$$I_j = \frac{V_j}{Z_{jj,new} + z_f} = -I_{fj}. \tag{2.3}$$

The voltage at bus *j* is

$$V_j = z_f I_{fj} - V_f. \tag{2.4}$$

The three phase fault current at bus *j* can be evaluated by substituting (2.4) into (2.3) [32],

$$I_{fj} = \frac{V_f}{\left(Z_{jj,orig} - \frac{Z_{jk,orig}^2}{Z_{kk,orig} + Z_{gen}} \right) + z_f} \tag{2.5}$$

where Z_f is the fault impedance and V_f is the prefault voltage from a load flow calculation. The diagonal elements of the new bus impedance matrix are used to calculate the fault current at the faulted bus, and the off-diagonal elements are required to calculate the change in voltage and current flows in the system during the fault.

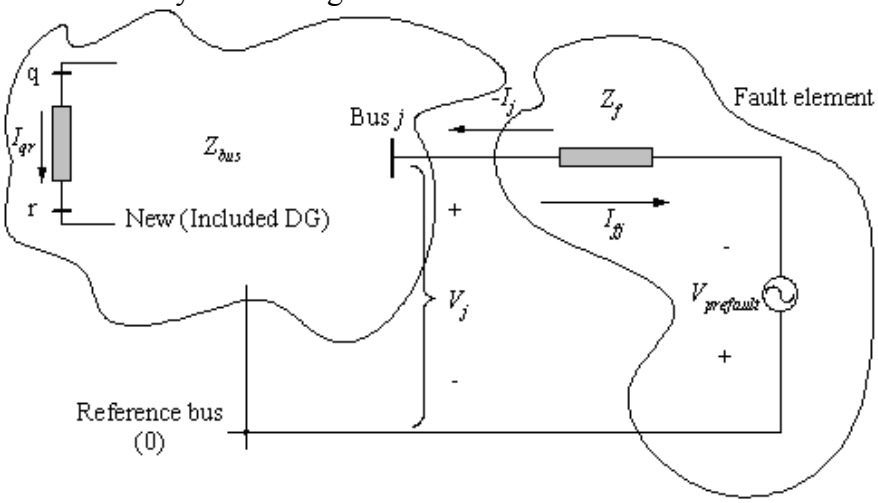

Figure 2.2 Fault occurs at bus *j* in the system including the new DG from Nimpitiwan [32]

During the fault at bus *j*, the change in voltage ($\Delta|V|$) can be calculated by the bus impedance matrix equations,

$$\begin{bmatrix} \Delta V_1 \\ \Delta V_2 \\ \Delta V_j \\ \text{M} \\ \Delta V_n \end{bmatrix} = \begin{bmatrix} -\frac{Z_{1j}}{Z_{jj,new}} V_f \\ -\frac{Z_{2j}}{Z_{jj,new}} V_f \\ -\frac{Z_{jj}}{Z_{jj,new} + z_f} V_f \\ \text{M} \\ -\frac{Z_{nj}}{Z_{jj,new}} V_f \end{bmatrix} \tag{2.6}$$

or the voltage during a fault can be obtained as,

$$V_i = \begin{bmatrix} V_f - \dfrac{Z_{1j}}{Z_{jj,new}} V_f \\ V_f - \dfrac{Z_{2j}}{Z_{jj,new}} V_f \\ V_f - \dfrac{Z_{jj}}{Z_{jj,new} + z_f} V_f \\ \text{M} \\ V_f - \dfrac{Z_{nj}}{Z_{jj,new}} V_f \end{bmatrix} \qquad i = 1,2,\ldots, n.$$

The current flowing from bus q to r, as shown in Figure 2.2, is

$$I_{qr} = \frac{V_q - V_r}{\lambda_{qr}} = \frac{V_f (Z_{qk} - Z_{rk})}{\lambda_{qr} (Z_{jj,new} + z_f)} \tag{2.7}$$

where ℓ_{qr} is the primitive line impedance from bus q to bus r, and z_f is the fault impedance.

Equation (2.5) can be applied to examine the fault current consequences of installing a new DG. In order to calculate the new impedance matrix, a model of the DG should be known. These models may be complicated due to complex controls, or may be unknown. Some degree of engineering judgment may be needed to obtain an approximate model. There are many technologies for distributed generation beyond conventional synchronous generators. Analysis of the fault current in the case of a new DG in the system requires knowledge of the model such as indicated by [13]-[16].

In the case where several new DGs are installed, for example at bus k and m, system equation including the new DGs is,

$$\begin{bmatrix} V_{orig} \\ \hline V_k \\ V_m \end{bmatrix} = \left[\begin{array}{ccccc|cc} & & Z_{bus,orig} & & & Z_{1k} & Z_{1m} \\ & & & & & Z_{2k} & Z_{2m} \\ & & & & & \text{M} & \text{M} \\ & & & & & Z_{nk} & Z_{nm} \\ \hline Z_{k1} & Z_{k2} & \Lambda & & Z_{kn} & Z_{kk} & Z_{km} \\ Z_{m1} & Z_{m2} & \Lambda & & Z_{mn} & Z_{mk} & Z_{mm} \end{array}\right] \begin{bmatrix} I_{orig} \\ \hline I_k \\ I_m \end{bmatrix}.$$

Buses k and m are the locations of the two DGs. The assumption of two DGs added will be generalized later. Applying Kron's reduction, therefore,

$$[Z_{bus,new}] = [Z_{bus,orig}] - [Z_{col,DGs}][Z_{common}]^{-1}[Z_{row,DGs}], \tag{2.8}$$

where

$$Z_{col,DGs} = \begin{bmatrix} Z_{1k} & \Lambda & Z_{1m} \\ Z_{2k} & \Lambda & Z_{2m} \\ \text{M} & \text{M} & \text{M} \\ Z_{nk} & \Lambda & Z_{nm} \end{bmatrix},$$

$$Z_{common} = \begin{bmatrix} Z_{kk} & & Zmk \\ & \text{O} & \\ Zkm & & Z_{mm} \end{bmatrix},$$

$$Z_{row,DGs} = \begin{bmatrix} Z_{k1} & Z_{k2} & \Lambda & Z_{kn} \\ \text{M} & \text{M} & \text{M} & \text{M} \\ Z_{m1} & Z_{m2} & \Lambda & Z_{mn} \end{bmatrix}.$$

Note that n is number of buses in the system not counting k and m, and k and m are DG buses. After calculating new Z_{bus} matrix, the new fault current is given by Equation (2.3).

References [16]-[18] propose an application of ANNs to analyze faults from system waveforms. The applicability in the case of the presence of DGs in the system is unknown, and the concept is offered as a point of interest only.

2.3 An illustrative example

Modify the bus impedance matrix of a simple 4-bus network to account for the connection of two new DGs at bus 3 and 4. As shown in Figure 2.3, the impedances of DGs installed at bus 3 and 4 are $j0.5$ and $j1.0$, respectively. The bus impedance matrix of original system is (using Matlab notation $i = \sqrt{-1} = j1$),

$$\text{Zbus} = \begin{pmatrix} 0.717\text{i} & 0.610\text{i} & 0.533\text{i} & 0.580\text{i} \\ 0.610\text{i} & 0.732\text{i} & 0.640\text{i} & 0.697\text{i} \\ 0.533\text{i} & 0.640\text{i} & 0.717\text{i} & 0.670\text{i} \\ 0.580\text{i} & 0.697\text{i} & 0.670\text{i} & 0.763\text{i} \end{pmatrix}.$$

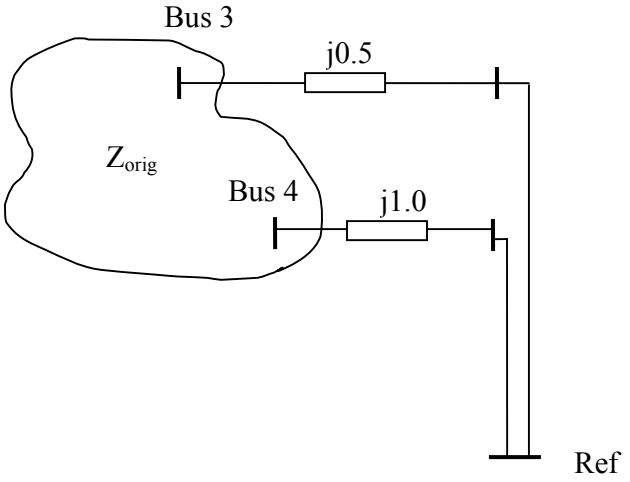

Figure 2.3 A 4-bus system with new DGs at bus 3 and 4

Apply Equation (2.8),

$$Z_{bus,new} = Zbus - \begin{bmatrix} j0.533 & j0.580 \\ j0.640 & j0.670 \\ j0.717 & j0.670 \\ j0.670 & j0.763 \end{bmatrix} \begin{bmatrix} j0.717 + j0.5 & j0.670 \\ j0.670 & j0.763 + j1 \end{bmatrix}^{-1} \begin{bmatrix} j0.533 & j0.640 & j0.717 & j0.670 \\ j0.580 & j0.670 & j0.670 & j0.763 \end{bmatrix}$$

$$Z_{bus,new} = \begin{bmatrix} j0.424 & j0.258 & j0.163 & j0.206 \\ j0.258 & j0.310 & j0.195 & j0.247 \\ j0.163 & j0.195 & j0.240 & j0.197 \\ j0.206 & j0.247 & j0.197 & j0.283 \end{bmatrix}$$

Assume that the prefault voltage of the system is 1 p.u. at each bus. The three phase fault current can be calculated as,

$$I_j = \frac{V_j}{Z_{jj,new} + z_f} \cdot$$

Table 2.1 shows the results of replacing diagonal elements of $Z_{bus,new}$ into Equation (2.3) and the change of fault currents after installing new DGs.

Table 2.1 Summary of calculation for the simple 4-bus system shown in Figure 2.3

Bus	Fault current before installing DG (p.u.)	Fault current after installing DG (p.u.)	$\Delta\lvert I_f \rvert$ (%)
1	1.39	2.36	96.8 %
2	1.37	3.23	135.7 %
3	1.39	4.17	200 %
4	1.31	3.53	169.5 %

As shown in Table 2.1, from the simple 4-bus system represented by Z_{bus} matrix, the fault currents are increased after installing new DGs into the system. Note that, the change of fault current, $\Delta\lvert I_f \rvert$, spreads through out the system. From Equation (2.5), the change of fault current depends on the stator transient reactance (Z_{gen}) of DGs.

As mentioned in Chapter 1, the consequences of the change of fault current might result in the requirement of upgrading the system protection, especially circuit breakers and setting of protective relays. True conclusion can not be drawn from the illustrative example above; however, larger systems and actual systems can be used as test beds to develop conclusions. The analysis in this chapter is applied to analyze a larger 27-bus system in Chapter 3. A simple technique to assess the severity of the increase of fault current is presented in Chapter 4 by the least squares method.

3. Factors that Affect the Severity of Fault Currents: Illustrative Case Studies

3.1 Introduction

In this chapter, the increase of fault currents due to the addition of DGs are investigated by applying the theory discussed in Chapter 2. The investigation is done using a test bed. The objective is to illustrate the calculation technique, obtain typical values for a 69 kV (subtransmission, networked) – 12 kV (distribution, radial) system. A large electric utility company in Phoenix, AZ supplied a representative subtransmission – distribution system. Salt River Project (SRP) supplied the Thunderstone system shown in Figure 3.1 as a test bed. The system data are given in Appendix A. The Thunderstone system is connected to 230 kV transmission system at bus Thunder1, considered as the system slack bus. The voltage level at 230 kV from slack bus is stepped down to 69 kV at The Thunderstone substation, shown in Figure 3.1. The taps of substation transformer at 230 kV and the 12 kV distribution transformers usually operate higher than 1.0 p.u. to reduce the effect of voltage drop in the distribution level. The Thevenin equivalent impedance of 230 kV bus is 0.75728+*j*6.183 ohm per phase. Note that capacitors are installed at the load sites to improved power factors. Results of capacitors are included in the load data shown in Table A.2. The results of investigation by applying the theory in Chapter 2 are analyzed and compared with the results from the power system analysis software called "PowerWorld" [33]. All parameters are used to form the bus impedance matrix in Matlab by applying the bus impedance building technique [1]. Three phase fault currents in the system can be calculated by utilizing the bus impedance matrix as given by Equation (2.8).

At this point, a new index is suggested for the purpose of quantifying fault current system-wide. The severity of increase of fault currents in the system can be indicated by a new index, the Average Change of Fault current (*ACF*),

$$ACF = \frac{\sum_{\substack{n=1 \\ n \neq bus\ with\ DG}}^{nbus} \left| \frac{I_{f,n} - I_{fDG,n}}{I_{f,n}} \right| \times 100}{(nbus - nDG - 1)} \quad , \tag{3.1}$$

where $I_{f,n}$ is the fault current at bus n before installing new DG, $I_{fDG,n}$ is the fault current at bus n after installing new DGs into the system, nDG is the bus with DG, and $nbus$ is the total buses in the system. Note that $\left| \frac{I_{f,n} - I_{fDG,n}}{I_{f,n}} \right| \times 100$ is the percent change of amplitude of the fault currents. Although ACF does not show individual fault currents, it does give an index of system-wide impact of DGs on fault current. It is suggested to use ACF as a system-wide measure, but it is not suggested to replace the standardized methods to represent individual bus fault currents. Normally, owner of new DGs have to upgrade the fault current interrupting capability of the local circuit breaker. However, the local DG owner has no access to circuits beyond their own PCC with the utility owned system. The cost and responsibility of upgrading equipment in the utility company domain seemingly must fall to the utility company. In a deregulated environment, all costs need to be "assigned" to the sectors that produce those costs. Equation (3.1) is offered as a suggestion as a basis of assigning upgrade costs.

3.2 Fault analysis for the Thunderstone system

The Thunderstone system is investigated by installing new DGs into the system at various buses, such as Cameron2, Signal3, Sage3 and Seaton2. All DGs are installed with the same size as their local loads. That is, the DG is sized to support the local load at 100%.

The factors that play an important role in the increase of fault current in the system are:

- the number and locations of DGs
- the size of DGs
- the status of Automatic Voltage Regulator (AVRs) of the DGs
- the impedance of the DGs.

The following cases show the consequences of the increase in the magnitude of three-phase fault current in the Thunderstone system. Analysis in the next section is performed by assuming that all DGs are synchronous generators and loads in the system at 12 kV buses are considered as constant power loads.

Case 3.1 Number and locations of DGs

In Case 3.1, DGs are installed in Thunderstone system at various locations: Cameron2, Signal3, Sage3 and Seaton2. All DGs are assumed to have the same internal impedance (z_{DG}), 0.005+*j*1.2 per unit on a 100 MVA base. Both power and reactive power of each DG are controlled to serve only the local loads. For purpose of these studies, the DG penetration level is defined as,

$$\frac{Total\ MVA\ served\ by\ DGs}{Total\ Load + System\ Losses} \times 100\ \%.$$

The results of increasing the penetration level into the system is captured using the ACF and these results are shown in Table 3.1. Figures 3.1 to 3.4 show the severity of the increase of the fault current. Note that the shaded areas correspond to the higher change of fault current. These areas spread out when penetration level is increased.

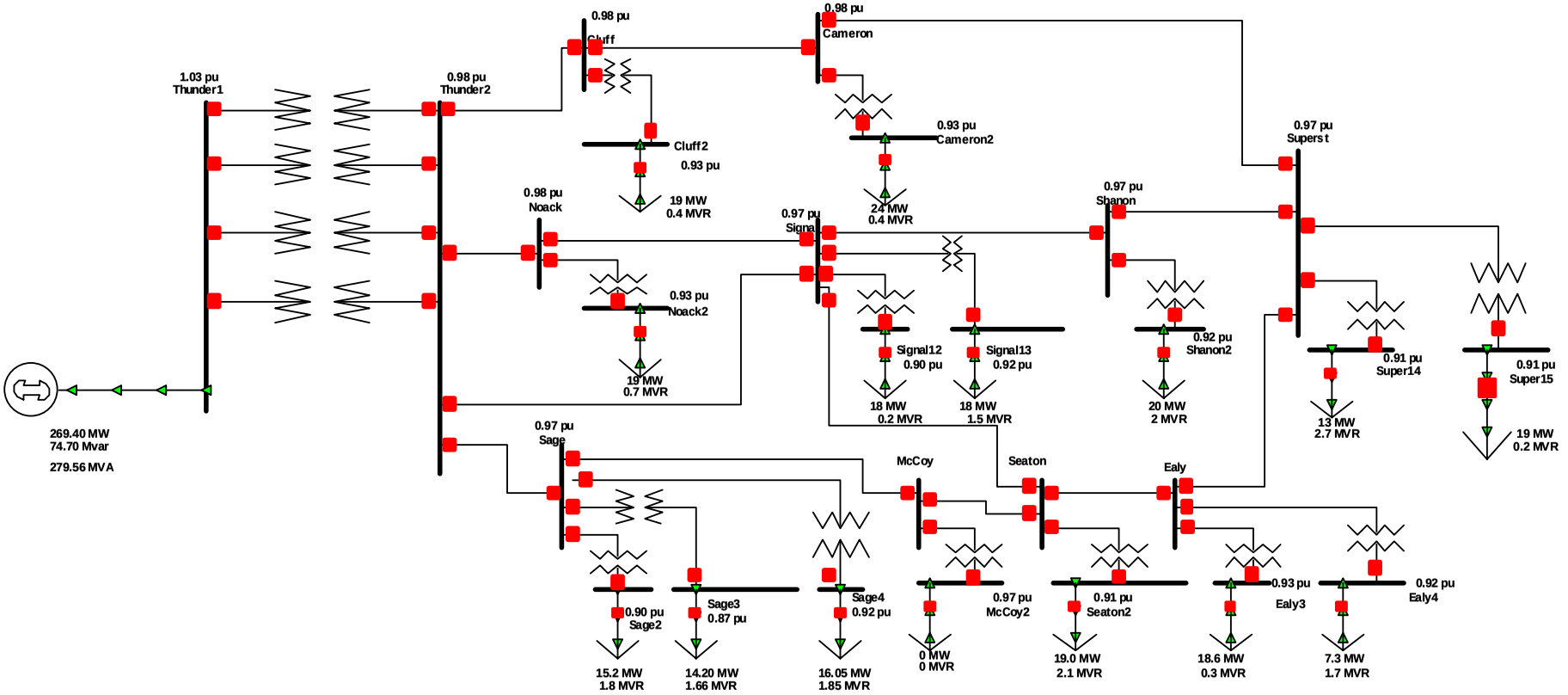

Figure 3.1 Thunderstone 69 kV transmission system

Table 3.1 Results of installing new DGs at various number and locations in the Thunderstone system Case 3.1

Location of new DG	DG (MV A)	Power factor of DG	Penetration level (percent)	Average Change of Fault current, ACF (percent)	Maximum change of I_f (percent)	Bus with maximum change of I_f
Cameron2	25	0.9998	9.2	1.4	3.02	5
Cameron2 Signal3	25 19.1	0.9998 0.99647	16.4	2.7	3.94	5
Cameron2 Signal3 Sage3	25 19.1 20.2	0.9998 0.99647 0.994	24.1	4.3	5.48	21
Cameron2 Signal3 Sage3 Seaton2	25 19.1 20.2 15.1	0.9998 0.99647 0.994 0.9932	29.8	5.5	6.71	21

Case 3.2 Automatic Voltage Regulator (AVR) operative / inoperative

An AVR is a local automatic control to hold generator terminal voltage magnitude $|V|$ fixed. When a generator is on AVR control, the reactive power output of the generator is varied automatically in order to maintain the regulated bus voltage magnitude at a specific controlled value. The control of reactive power output is accomplished by varying the field excitation of the synchronous generator, and the V_f is control output of the AVR. The AVR plays an important role in calculating the increase of fault currents in the system due to DG installation.

Case 3.2 (see Appendix B for a tabulation of all case study conditions) shows the comparison between installing DG with and without AVR control into the Thunderstone system. In this case, DGs are installed at Seaton, Cameron2, Signal13 and Sage3. All DGs generate 20 MW to serve the local loads as shown in Figure 3.6.

Note that the DG bus without the AVR controller might have voltage level higher than one per unit. This depends on the reactive power generated by the DG. Conversely, in case that the DG is equipped with an AVR, the voltage level at the bus with the DG is normally controlled at one per unit. For this reason, the fault current of the system without applying the AVR control tends to have the higher fault current. Comparisons between the systems with turning AVR control on or off are shown in Figure 3.7.

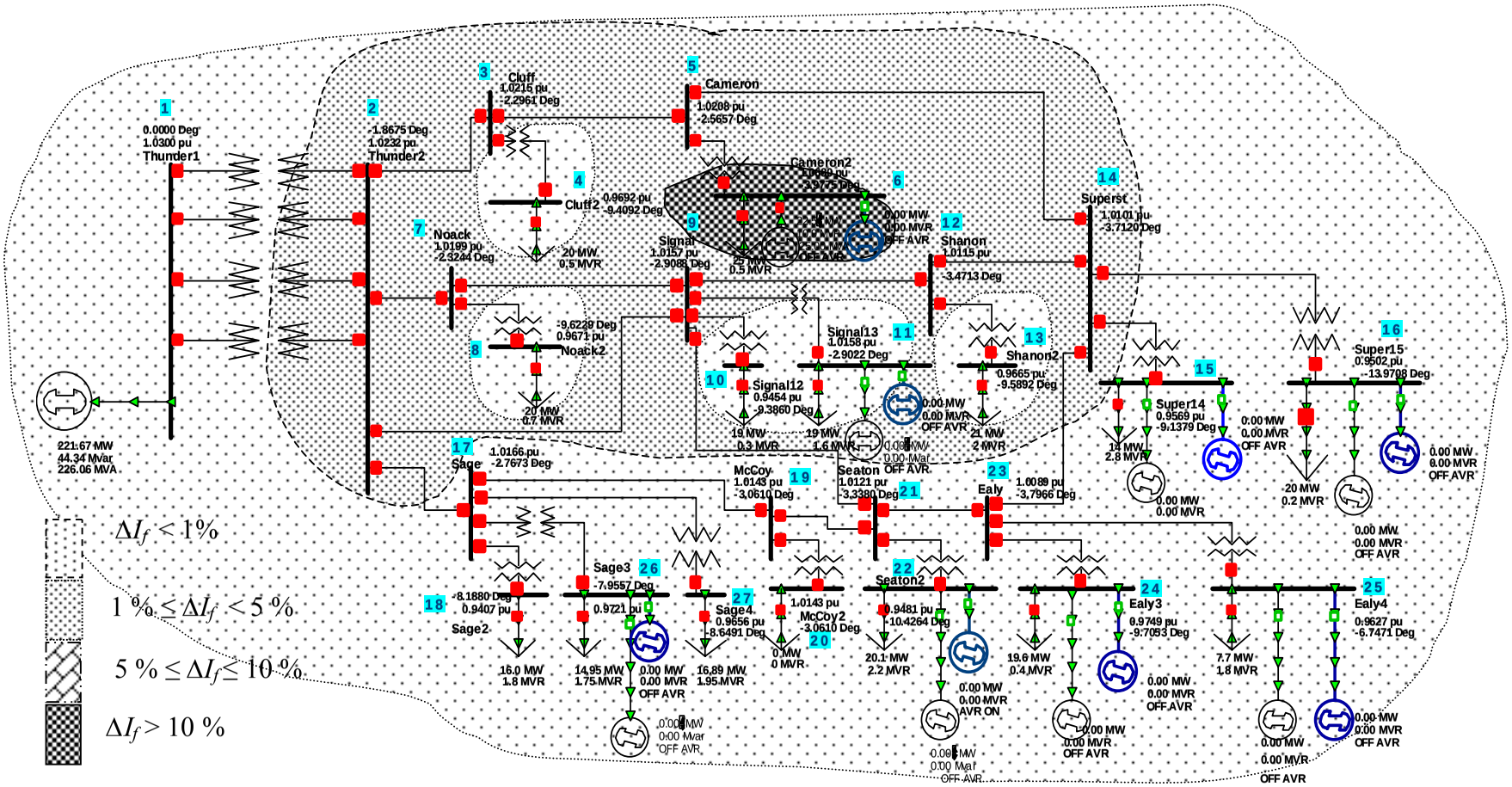

Figure 3.2 The change of fault current of the system after installing a new DG at Cameron2, Case 3.1

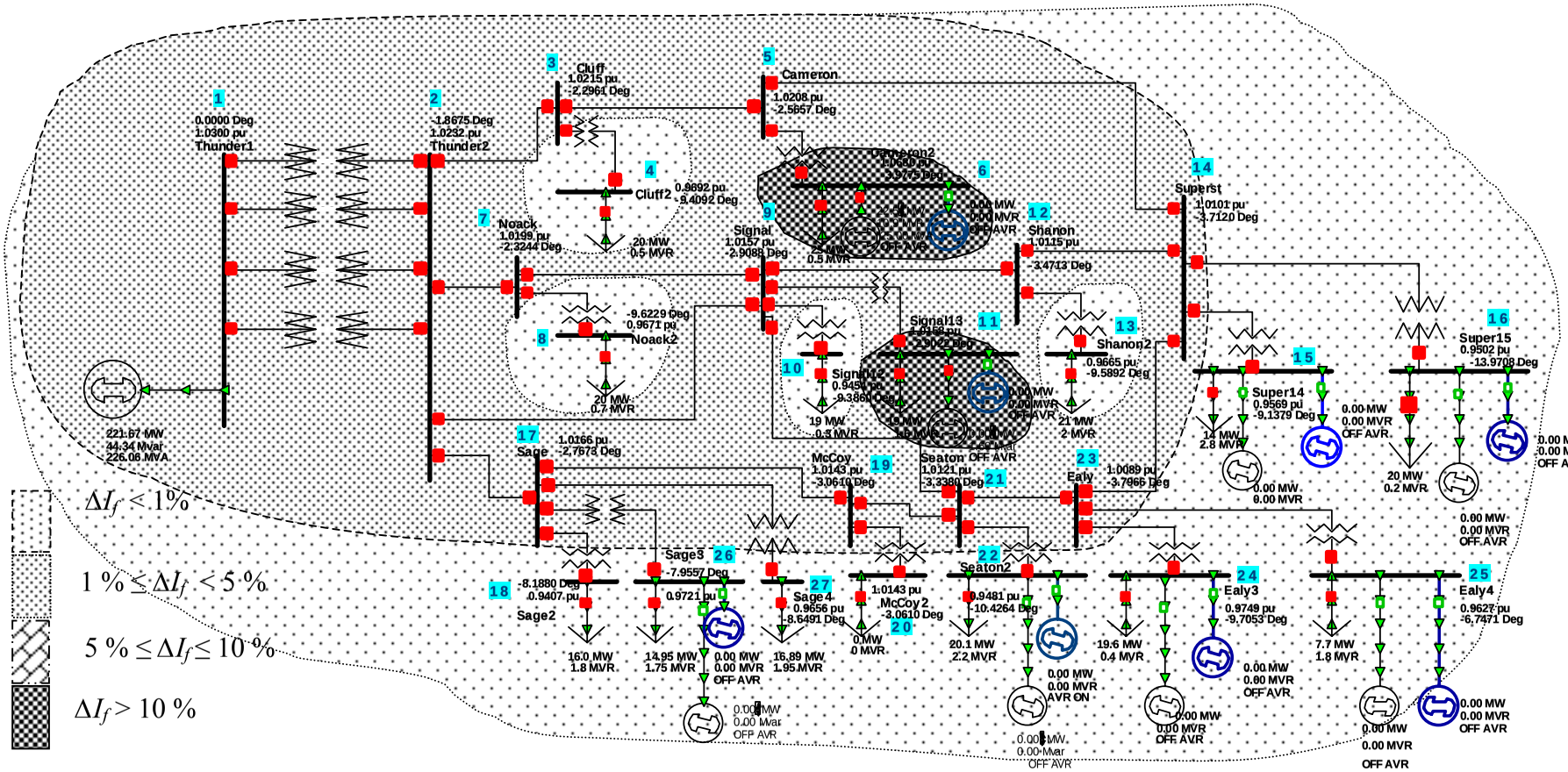

Figure 3.3 The change of fault current of the system after installing a new DG at Cameron2 and Signal13, Case 3.1

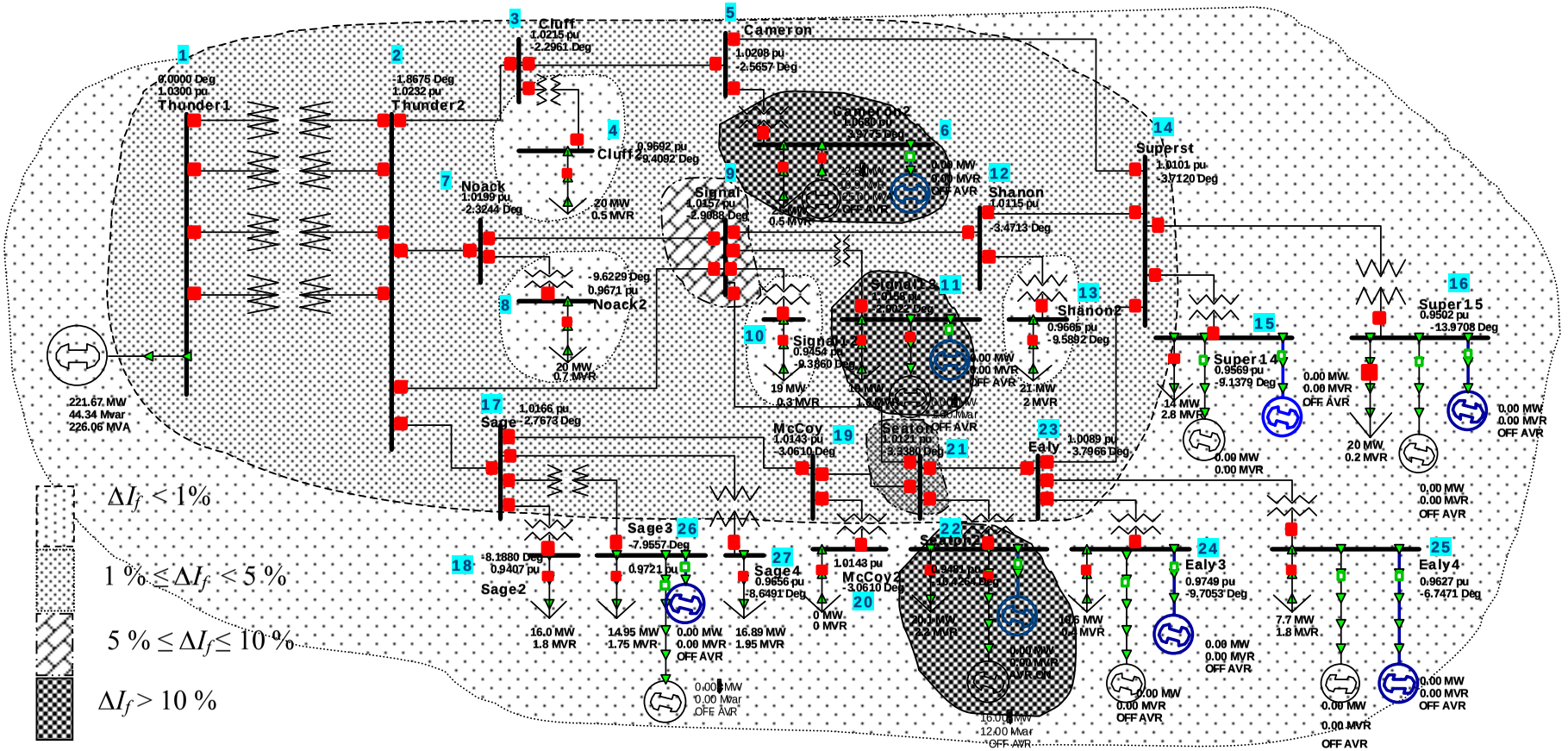

Figure 3.4 The change of fault current of the system after installing a new DG at Cameron2, Signal13 and Seaton2, Case 3.1

Case 3.3 Impedance of DGs

The internal impedance of a DG is a significant factor in the calculation of increased of fault current. In Case 3.3, four DGs are installed at the same positions as Case 3.1. However, the reactance of each DG is varied from 0.5 to 1.5 per unit (on the bases dictated by the DG ratings). Figure 3.8 shows the result of varying the stator transient reactance of DGs. For Case 3.3, all DG transient impedance were increased equally. Note that decreasing of the transient impedance of the DGs increases the ACF in the system.

3.3 Conclusions

The fault analysis of the Thunderstone 27-bus system is performed by applying the analysis of Chapter 2. The factors which affect the severity of the change of fault current, such as number/location, AVR on/off and impedance of DGs, are discussed in Cases 3.1 to Case 3.3, respectively.

In this chapter, the severity of increase in fault current is represented by a new index called "ACF". The ACF index is offered as a new system-wide measure of the change in fault current in the system. This index may be applied as a part of the allocation of cost of upgrading the system.

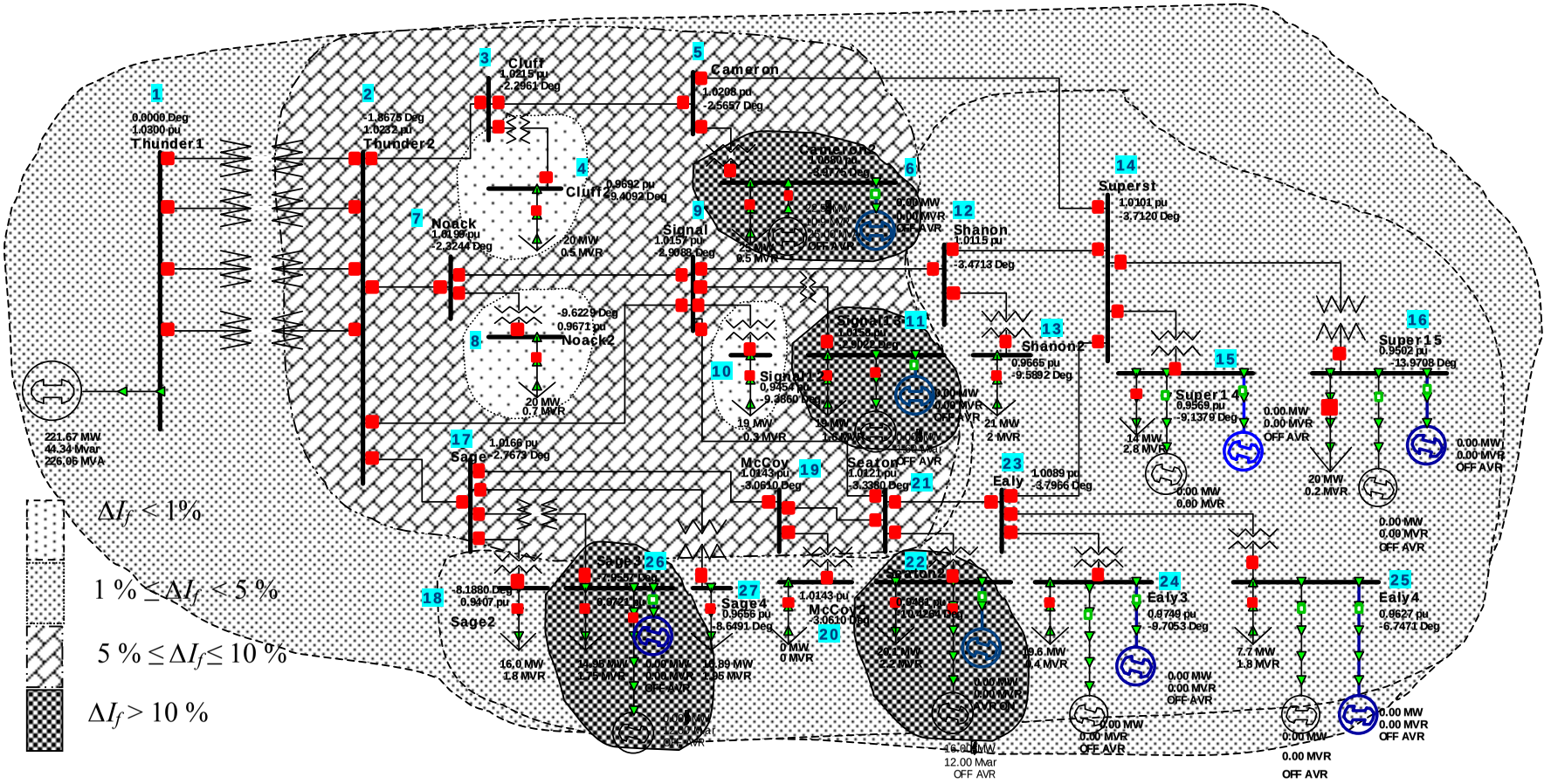

Figure 3.5 The change of fault current of the system after installing a new DG at Cameron2, Signal13, Seaton2 and Sage3, Case 3.1

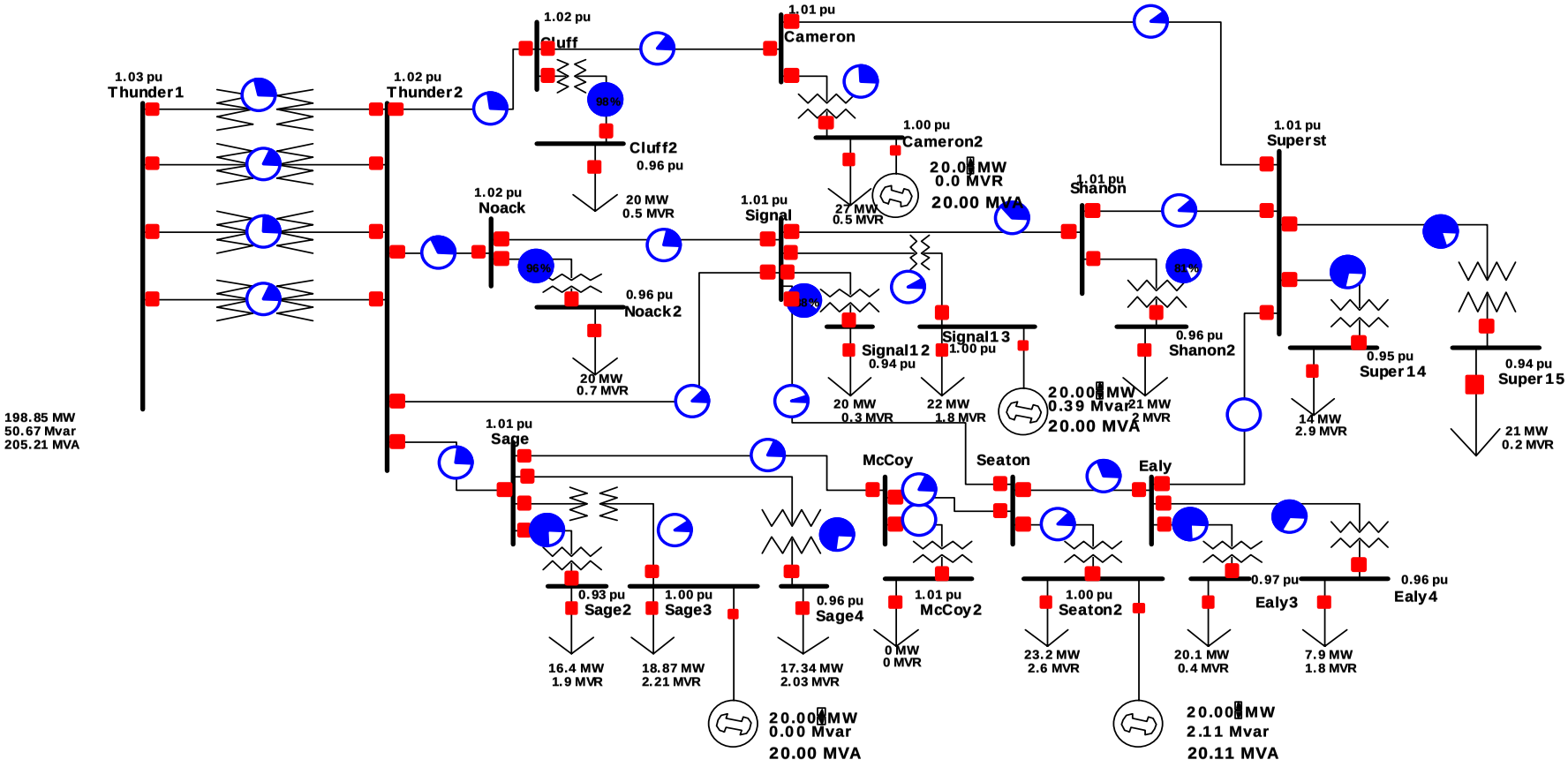

Figure 3.6 Thunderstone system with new DGs at Seaton, Cameron2, Signal3 and Sage3, Case 3.2

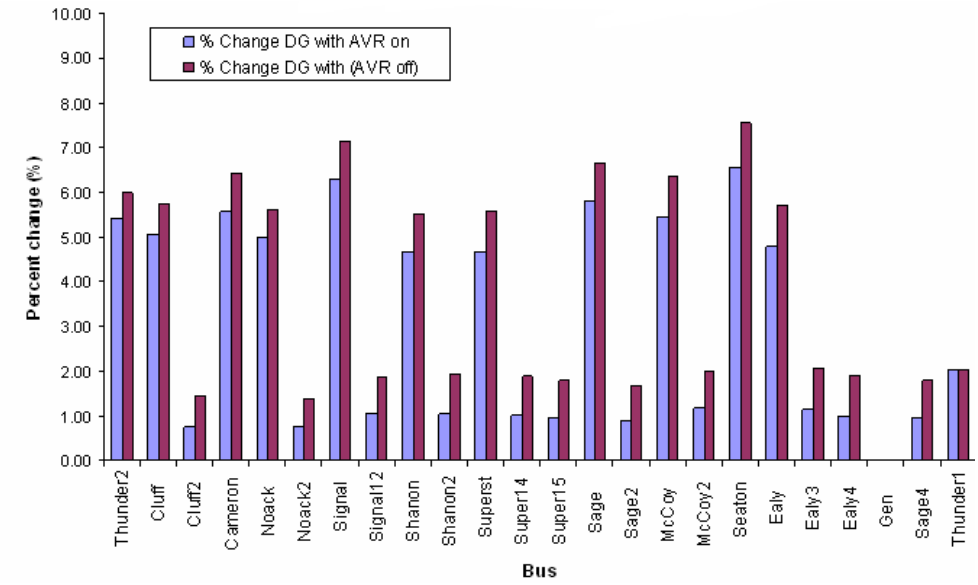

Figure 3.7 Increasing of fault current as a result of turning AVR control on/off, Case 3.2

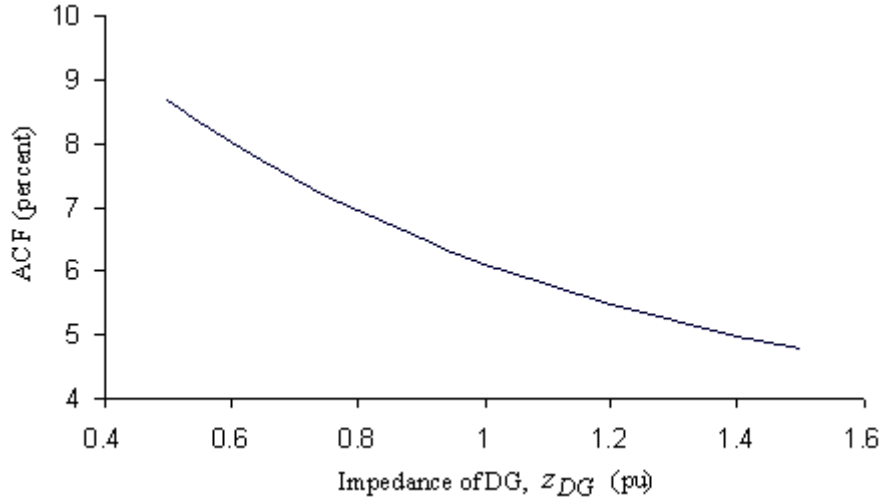

Figure 3.8 The increasing of fault current dues to varying the reactance of DGs, Case 3.3

4. Fault Calculation by the Least Squares Method

4.1 Introduction

In order to assess the severity of increasing fault current in the system after installing DGs, a fault current analysis is done. This procedure is standardized and considered critical. The fault current analysis presented in Chapter 3 requires a load flow study calculation prior to applying Equation (2.3). Fault currents from Equation (2.3) give accurate results within the assumptions made; however, the calculation procedure is complicated and requires a long process.

The ACF index discussed in Chapter 3 can be used to indicate the severity of the change in the fault current system-wide. This chapter proposes a least squares method for calculating the ACF. Note that the least squares method is also known as the weighed least-squares estimator or the maximum likelihood estimator. The details and derivations of the least squares method are presented in [35, 37, 38].

4.2 A least squares estimate of ACF

In Chapter 3, the ACF index was offered as a way to characterize fault current increase due to the addition of DG. The ACF index, however, is not simply calculated because several complex subprocedures must be done. One way to reduce complexity is to estimate ACF for a given system on the basis of several previously analyzed cases. Figure 4.1 shows the approach.

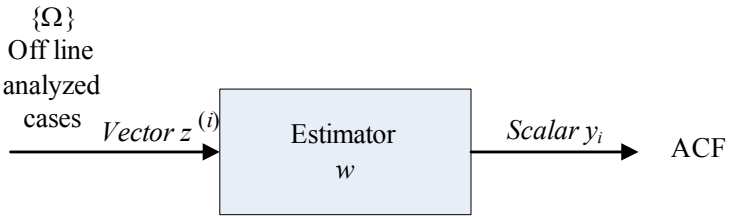

Figure 4.1 System diagram of the least square estimator

In Figure 4.1, offline, previously calculated cases are denoted as the set Ω. In each of the cases in Ω, a datum vector $z^{(i)}$ is used. The superscript (i) refers to the sample number. When the vector $z^{(i)}$ are arranged in a matrix, for all cases in Ω, the matrix Z results. Similarly, the ACF resulting from the use of vector $z^{(i)}$ is denoted as the scalar value y_i. When all the case results in Ω are arranged in a matrix, the vector y results. The question of how y_i is related to $z^{(i)}$ (for case i in Ω) is now considered. Let several functions of $z^{(i)}$ appear in a linear combination to generate y_i

$$y_i = \text{Linear combination } \{f_1(z^{(i)}), f_2(z^{(i)}), \ldots\}. \tag{4.1}$$

The f_k functions may be linear or nonlinear. But (4.1) is a *linear combination* of the $f_k(Z^{(i)})$ scalar functions.

At this point, relate the linear combination concept above to the calculation of ACF. Note that the ACF in case i (in Ω) depends on the impedance of newly added DGs at m different locations. That is, m DGs are added, and the ACF is calculated. Then

$$y_i = ACF_i = \sum_{j=1}^{k}\sum_{\lambda=1}^{m} w_{j,\lambda} f_j\left(z_{DG,\lambda}^{(i)}\right) . \tag{4.2}$$

In (4.2), $w_{j,\lambda}$ denotes the linear combination coefficients mentioned in Equation (4.1). The intent is that the y_i be a formula for ACF in case i, and the formula should have constant coefficients (i.e., the $w_{j,\lambda}$ coefficients are not a function of i). Also note in Equation (4.2) that k is the number of functions used in the linear combination shown in Equation (4.1). For example, if $k = 2$, y_i is a linear combination of $f_1(z_{DG,\lambda})$ and $f_2(z_{DG,\lambda})$ for all newly added DGs.

Consider of cases in the sample ensemble Ω. That is, in Equation (4.2), $i = 1, 2,\ldots, q$. From the vector y as a q–vector of calculated ACF values in each of the q cases in Ω. Then, the method of minimum least squares is to minimize the scalar residual r,

$$r^2 = \left(y_i - \sum_{j=1}^{k}\sum_{\lambda=1}^{m} w_{j,\lambda} f_j(z_{DG,\lambda}^{(i)}) \right)^2 . \tag{4.3}$$

Note that when $r = 0$, all ACF values in Ω calculated by (4.2) agree with the correct (full calculations) values y_i. The $w_{j,\lambda}$ coefficients may be arranged in a vector as follows

$$w = \begin{bmatrix} w_{1,1} \\ w_{1,2} \\ w_{1,3} \\ \text{M} \\ w_{1,m} \\ w_{2,1} \\ w_{2,2} \\ \text{M} \\ w_{2,m} \\ w_{3,1} \\ \text{M} \\ w_{k,m} \end{bmatrix} .$$

Thus, Equation (4.2) can be written as

$$ACF = y = Fw \tag{4.4}$$

and the least squares estimate of the vector of linear combination coefficients, $\hat{w}$, is

$$\hat{w} = F^{+} y \tag{4.5}$$

where F^{+} denotes the pseudoinverse. For this case, F^{+} is $\left(F'F\right)^{-1}F'$ [35, 37], and F is a q by mk matrix,

$$F = \begin{array}{c} \longleftarrow\ mk\ \longrightarrow \\ \left.\begin{array}{c} \uparrow \\ q \\ \downarrow \end{array}\right. \end{array} \begin{bmatrix} f_1(z_{DG,1}^{(1)}) & f_1(z_{DG,2}^{(1)}) & \Lambda & f_1(z_{DG,m}^{(1)}) & f_2(z_{DG,1}^{(1)}) & \Lambda & f_k(z_{DG,m}^{(1)}) \\ f_1(z_{DG,1}^{(2)}) & & & \Lambda & & & f_k(z_{DG,m}^{(2)}) \\ \text{M} & & & \text{O} & & & \text{M} \\ f_1(z_{DG,1}^{(q)}) & & & \Lambda & & & f_k(z_{DG,m}^{(q)}) \end{bmatrix} \tag{4.6}$$

where $z_{DG,a}^{(b)}$ refers to the impedance of a newly added DG at bus a for case b in $\{\Omega\}$. References [1, 2, 35, 38] document the unbiased least squares approach indicated by Equation (4.5). To review, Equation (4.5) is

$$\hat{w} = \text{ Estimate of } w$$
$$= F^{+} y \ .$$

where $\hat{w}$ is a mk vectors, y is q vector and F^{+} is q by mk matrix. To assist the reader in following the mathematics, Table 4.1 is offered.

In the foregoing, the general case of k terms is used to estimate ACF for each newly added DG bus. The selection of k and the functional forms of the f_j, $j = 1,\ldots, k$ terms in (4.2) need to be made.

In this application, the least squares estimator is applied to calculate the ACF of the system corresponding to the impedance of DGs as shown in Figure 4.1. The unknown system can be modeled as the following functions that are linear in the w terms,

First order ($k = 1$): $$ACF_i = y_i = \sum_{\lambda=1}^{m} w_{1,\lambda} \cdot \left| z_{DG,\lambda}^{(i)} \right| \qquad (4.7a)$$

Second order ($k = 2$): $$ACF_i = y_i = \sum_{\lambda=1}^{m} w_{1,\lambda} \cdot \left| z_{DG,\lambda}^{(i)} \right| + \sum_{\lambda=1}^{m} w_{2,\lambda} \cdot \left| z_{DG,\lambda}^{(i)} \right|^2 \qquad (4.7b)$$

Third order ($k = 3$):

$$ACF_i = y_i = \sum_{\lambda=1}^{m} w_{1,\lambda} \cdot \left| z_{DG,\lambda}^{(i)} \right| + \sum_{\lambda=1}^{m} w_{2,\lambda} \cdot \left| z_{DG,\lambda}^{(i)} \right|^2 + \sum_{\lambda=1}^{m} w_{3,\lambda} \cdot \left| z_{DG,\lambda}^{(i)} \right|^3 \qquad (4.7c)$$

Table 4.1 Dimensions of several quantities used in the least squares estimation of ACF

Quantity		Rows	Columns
r	Residual of the least squares estimation	1	1
y	Vector of output data from linear combination	mk	1
y_i	Value of ACF	1	1
$f_1, f_2, \ldots$	Functions used to approximate ACF	1	1
$z^{(i)}$	Vector of input data for estimate, case (i)	m	1
Z	Matrix of input data for estimate, all case	q	m
$w_{j\lambda}$	Element of vector w, linear combination coefficient	1	1
w	Linear combination coefficient	mk	1
F	Relationship matrix	q	mk
F^{+}	Pseudoinverse of relationship matrix	q	mk
$\hat{w}$	Estimate of linear combination coefficient	mk	1
m	Number of bus with possibly DG added	1	1
k	Order of the ACF model	1	1
q	Number of case in Ω	1	1

Reciprocal of $z_{DG,\lambda}$ ($k = 1$): $$ACF_i = y_i = \sum_{\lambda=1}^{m} w_{1,\lambda} \cdot \left| z_{DG,\lambda}^{(i)} \right|^{-1} \qquad (4.7d)$$

Reciprocal of $z_{DG,\lambda}$ squares ($k = 2$) :

$$ACF_i = y_i = \sum_{\lambda=1}^{m} w_{1,\lambda} \cdot \left| z_{DG,\lambda}^{(i)} \right|^{-1} + \sum_{\lambda=1}^{m} w_{2,\lambda} \cdot \left| z_{DG,\lambda}^{(i)} \right|^{-2} \qquad (4.7e)$$

Reciprocal of $z_{DG,\lambda}$ cubes ($k = 3$) :

$$ACF_i = y_i = \sum_{\lambda=1}^{m} w_{1,\lambda} \cdot \left| z_{DG,\lambda}^{(i)} \right|^{-1} + \sum_{\lambda=1}^{m} w_{2,\lambda} \cdot \left| z_{DG,\lambda}^{(i)} \right|^{-2} + \sum_{\lambda=1}^{m} w_{3,\lambda} \cdot \left| z_{DG,\lambda}^{(i)} \right|^{-3} \qquad (4.7f)$$

where $z_{DG,\lambda}^{(i)}$ is the impedance of the added DGs in case *i* and $w_{1,\lambda}$, $w_{2,\lambda}$ and $w_{3,\lambda}$ is the coefficient of the first, the second and the third order, respectively.

Calculation of the linear coefficient vector, $w_{j,\lambda}$, used in Equation (4.5) is comparable to the parameter estimation techniques [35, 37]. Equation (4.4) from the least squares method can be written in the state estimation sense as,

$$Hx = z \ ,$$

where *x* or the coefficients of linear function is equivalent to the coefficient vector, *w*, the incident matrix *H* is equivalent to the relationship matrix *F* shown in Equation (4.6) and z or the vector of measured values is equivalent to the vector of the ACF.

4.3 Application of the least squares method to the Thunderstone system, Case 4.1

In this example, Case 4.1, the Thunderstone system shown in Figure 3.1 is used to illustrate the proposed least squares method. Note that the conditions of all the tests appear in Appendix B. By applying the reciprocal of $z_{DG,\lambda}$ cubes model, shown in Equation (4.7f),

$$ACF_i = y_i = \sum_{\lambda=1}^{m} w_{1,\lambda} \cdot \left| z_{DG,\lambda}^{(i)} \right|^{-1} + \sum_{\lambda=1}^{m} w_{2,\lambda} \cdot \left| z_{DG,\lambda}^{(i)} \right|^{-2} + \sum_{\lambda=1}^{m} w_{3,\lambda} \cdot \left| z_{DG,\lambda}^{(i)} \right|^{-3} , \qquad (4.8)$$

the coefficient vector, *w*, is calculated from the database which are generated randomly from the fault calculation program in Matlab. The database composes impedance of DGs and ACFs of the Thunderstone system. Assume that the DGs are installed at 6 locations: Cameron2, Signal3, Seaton2, Ealy3, Ealy4 and Sage3. The transient impedances of each DG are shown in Table 4.2.

Table 4.2 List of the buses with new DG in Case 4.1

Bus name	Transient impedance of the DG* (p.u.)
Cameron2 (6)	0.005 + *j*0.81
Signal3 (11)	0.005 + *j*0.90
Seaton2 (22)	0.005 + *j*0.83
Ealy3 (24)	0.005 + *j*0.85
Ealy4 (25)	0.005 + *j*0.92
Sage3 (26)	0.005 + *j*0.84

*Assumed values, for Case 4.1

The coefficient vector of the model is calculated by applying Equation (4.5). Note that the coefficient vector, *w*, can be separated into *k* groups depending on the order of each model. For example, in the reciprocal of $z_{DG,\lambda}$ cubes ($k = 3$), the first order coefficient of the coefficient vector, $w_{1,\lambda}$, is *m* by one sub-vector. For this reason, the coefficient vector, *w*, is *mk* by one vector. The coefficient vector, *w*, of the Thunderstone system is,

$$w = \begin{bmatrix} w_{1,\lambda} \\ w_{2,\lambda} \\ w_{3,\lambda} \end{bmatrix},$$

where

$$w_{1,\lambda} = \begin{bmatrix} 2.2048 \\ 2.5609 \\ 1.7878 \\ 2.3637 \\ 2.3148 \\ 2.7164 \\ 2.4916 \\ 2.3671 \\ 2.3834 \\ 2.6878 \\ 2.8195 \\ 2.8508 \\ 2.3576 \\ 2.2561 \end{bmatrix}, \; w_{2,\lambda} = \begin{bmatrix} -1.1148 \\ -1.2409 \\ -0.8427 \\ -1.1276 \\ -1.1037 \\ -1.1208 \\ -1.1090 \\ -1.1408 \\ -1.2601 \\ -1.2799 \\ -1.1144 \\ -1.4519 \\ -1.2003 \\ -1.1449 \end{bmatrix} \text{ and } \; w_{3,\lambda} = \begin{bmatrix} 0.2317 \\ 0.2641 \\ 0.1711 \\ 0.2298 \\ 0.2259 \\ 0.2100 \\ 0.2113 \\ 0.2252 \\ 0.2692 \\ 0.2643 \\ 0.2006 \\ 0.2991 \\ 0.2523 \\ 0.2447 \end{bmatrix}.$$

The impedance of the added DGs in this case is

$$|z_{DG}| = \begin{bmatrix} 0 & 0.81 & 0 & 0 & 0.90 & 0 & 0 & 0 & 0 & 0.83 & 0.85 & 0.92 & 0.84 & 0 \end{bmatrix}.$$

The ACF of the system from Equation (4.7) is

$$ACF = y = \begin{bmatrix} 0.0000 \\ 1.2345 \\ 0.0000 \\ 0.0000 \\ 1.2500 \\ 0.0000 \\ 0.0000 \\ 0.0000 \\ 0.0000 \\ 1.2048 \\ 1.1765 \\ 1.0869 \\ 1.1905 \\ 0.0000 \end{bmatrix}^t \hat{w}_{1,\lambda} + \begin{bmatrix} 0.0000 \\ 1.5241 \\ 0.0000 \\ 0.0000 \\ 1.5624 \\ 0.0000 \\ 0.0000 \\ 0.0000 \\ 0.0000 \\ 1.4515 \\ 1.3840 \\ 1.1814 \\ 1.4172 \\ 0.0000 \end{bmatrix}^t \hat{w}_{2,\lambda} + \begin{bmatrix} 0.0000 \\ 1.8816 \\ 0.0000 \\ 0.0000 \\ 1.9530 \\ 0.0000 \\ 0.0000 \\ 0.0000 \\ 0.0000 \\ 1.7488 \\ 1.6282 \\ 1.2842 \\ 1.6871 \\ 0.0000 \end{bmatrix}^t \hat{w}_{3,\lambda} \qquad (4.9)$$

$$= 10.63\ \%.$$

Note that the ACF from the conventional fault calculation is 10.87 %. The error from the least squares estimator compared to the conventional fault calculation is 2.25 %. The accuracy of the least squares model can be measured by the norm of the scalar residual r_i,

$$\frac{\|r\|}{\|F\hat{w}\|} = \frac{\|y - F\hat{w}\|}{\|F\hat{w}\|} \text{ p.u. ,}$$

where y is the vector ACF from the conventional fault calculation (full calculation).

In this calculation, the least squares estimator is created from 500 cases. The impedances of DGs installed at 12-kV buses are generated randomly under the same base MVA. Among the model in Equation (4.7), the reciprocal of $Z_{DG,\lambda}$ cubes shown in Equation (4.7f) has the highest accuracy. Norm of the scalar residual of each model is shown in Table 4.3. The histogram of the residual from the least squares model is shown in Figure 4.2.

Table 4.3 Norm of residual of Case 4.1

Model	*Equation*	*Norm of residual**
First order	(4.7a)	0.135
Second order	(4.7b)	0.0432
Third order	(4.7c)	0.0127
Reciprocal of $\left\|z_{DG,\lambda}\right\|$	(4.7d)	0.046
Reciprocal of $\left\|z_{DG,\lambda}\right\|^2$	(4.7e)	0.00655
Reciprocal of $\left\|z_{DG,\lambda}\right\|^3$	(4.7f)	0.00119

* expressed as a fraction, e.g., 0.135 = 13.4%

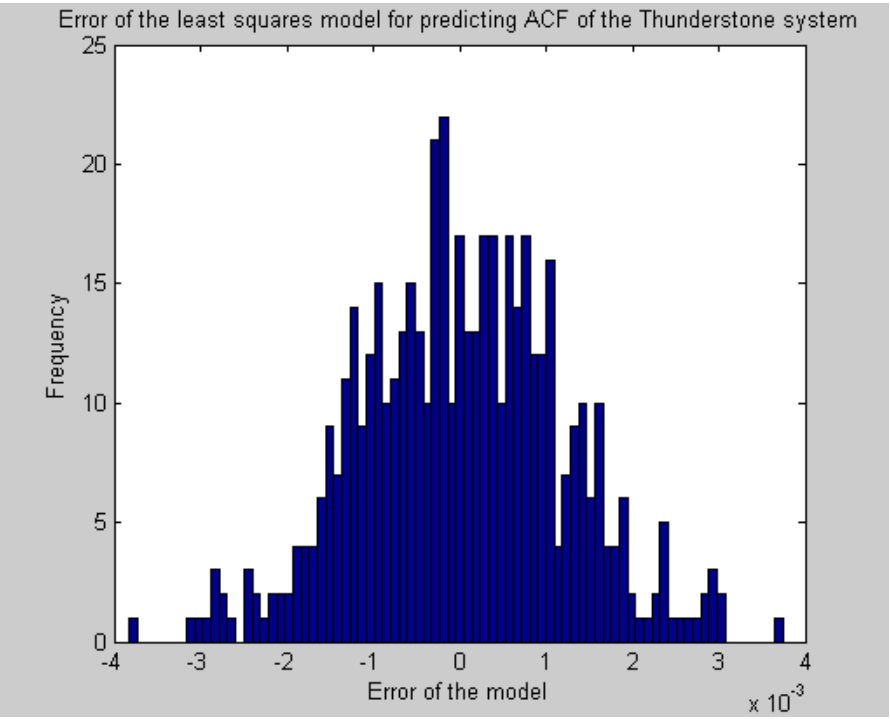

Figure 4.2 Residual of the least squares estimator, Case 4.1
(residual expressed as a fraction as in Table 4.3)

Note that Equation (4.9) can be independently written as 14 components according to fourteen 12 kV buses. Each component $ACF_{(bus)}$, called "Bus ACF", relates to the contribution of the DG to the total ACF. The plot of Bus ACF and the total ACF is shown in Figure 4.3. For instance, the contribution of the DG at bus 6 (Cameron2), 11 (Signal3), 22 (Seaton2), 24 (Ealy3), 25 (Ealy4) and 26 (Sage3) to ACF are

$$ACF_{(6)} = 2.5609 \cdot \frac{1}{\left|z_{DG,6}\right|} - 1.2409 \cdot \frac{1}{\left|z_{DG,6}\right|^2} + 0.2641 \cdot \frac{1}{\left|z_{DG,6}\right|^3}, \quad (4.10a)$$

$$ACF_{(11)} = 2.3148 \cdot \frac{1}{\left|z_{DG,11}\right|} - 1.1037 \cdot \frac{1}{\left|z_{DG,11}\right|^2} + 0.2259 \cdot \frac{1}{\left|z_{DG,11}\right|^3}, \quad (4.10b)$$

$$ACF_{(22)} = 2.6878 \cdot \frac{1}{\left|z_{DG,22}\right|} - 1.2799 \cdot \frac{1}{\left|z_{DG,22}\right|^2} + 0.2643 \cdot \frac{1}{\left|z_{DG,22}\right|^3}, \quad (4.10c)$$

$$ACF_{(24)} = 2.8195 \cdot \frac{1}{\left|z_{DG,24}\right|} - 1.1144 \cdot \frac{1}{\left|z_{DG,24}\right|^2} + 0.2006 \cdot \frac{1}{\left|z_{DG,24}\right|^3}, \quad (4.10d)$$

$$ACF_{(25)} = 2.8508 \cdot \frac{1}{\left|z_{DG,25}\right|} - 1.4519 \cdot \frac{1}{\left|z_{DG,25}\right|^2} + 0.2991 \cdot \frac{1}{\left|z_{DG,25}\right|^3}, \quad (4.10e)$$

$$ACF_{(26)} = 2.3576 \cdot \frac{1}{\left|z_{DG,26}\right|} - 1.2003 \cdot \frac{1}{\left|z_{DG,26}\right|^2} + 0.2523 \cdot \frac{1}{\left|z_{DG,26}\right|^3}. \quad (4.10f)$$

Figure 4.4 shows the comparison of the least squares estimator model and the conventional fault calculation. The accuracy of the least squares estimator when the DG transient impedance lies between $j0.5$ to $j1.5$ p.u., which is the usual range, is tolerable. Reasons for the error are:

- the historical data used to create the model ranges from $j0.5$ to $j1.5$ p.u.
- the pre-fault voltage is not included into the model. However, while calculating the historical data, the pre-fault voltages after installing DGs are updated and applied to the fault current calculation. For this reason, results of the pre-fault voltages after installing DGs are also included into the calculation of the ACF.

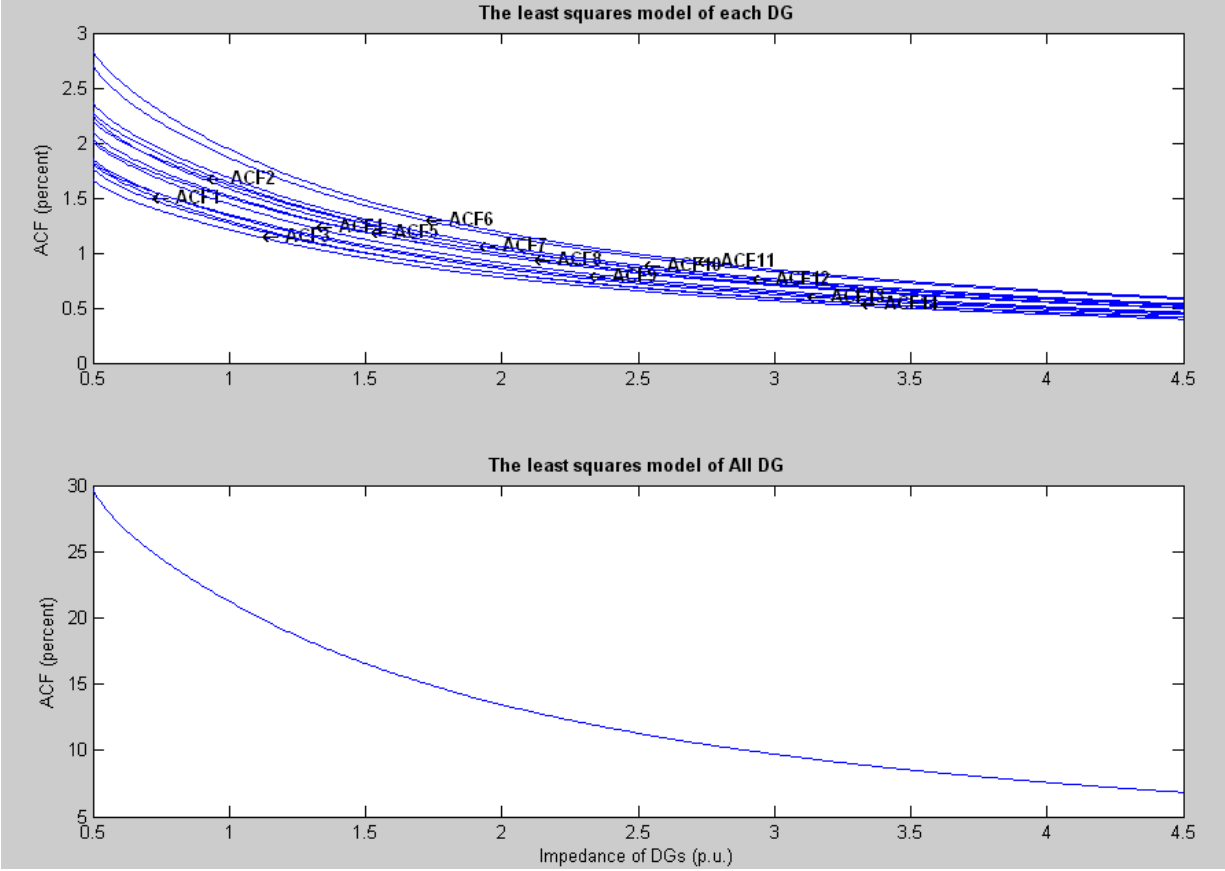

Figure 4.3 Plot of the bus ACF and the total ACF, Case 4.1

4.4 Confidence interval on the least squares estimator coefficient

Assuming that the residuals of the least squares estimator are normally and independently distributed with mean zero and variance, σ_r^2. The linear coefficient vector, $\hat{w}$, is normally distributed with the mean vector w and the covariance matrix

$\sigma_r^2 (F'F)^{-1}$. For the same reason, the marginal distribution of any least squares estimator, $\hat{w}_{j,\lambda}$, is normal with mean $w_{j,\lambda}$ and variance $\sigma_r^2 C_{jj}$, where C_{jj} is the *j*th diagonal element of the $(F'F)^{-1}$ matrix. Therefore, the 100(1-α) percent confidence interval for the least squares estimator coefficient $w_{j,\lambda}$ is [38]

$$\hat{w}_{j,\lambda} - t_{\alpha/2,n-p}\sqrt{\hat{\sigma}_r^2 C_{ii}} \le w_{j,\lambda} \le \hat{w}_{j,\lambda} + t_{\alpha/2,n-p}\sqrt{\hat{\sigma}_r^2 C_{ii}}, \qquad (4.11)$$

where $t_{\alpha/2,n-p}$ is the value from *t*-distribution, *n* is the number of all historical data, *p* is number of coefficient of the least squares estimator and $\hat{\sigma}_r^2$ is the estimation of variance of residual. The estimation of variance of residual, $\hat{\sigma}_r^2$ is,

$$\hat{\sigma}_r^2 = \frac{SS_{\mathrm{Res}}}{n-p} = \frac{y'y - \hat{w}'F'y}{n-p},$$

where SS_{Res} is the residual sum of squares [38].

Applying Equation (4.11), the 95 percent confidence intervals on the coefficient of the ACF model for the Thunderstone system, Case 4.1, are shown in Table 4.4

4.5 Confidence interval estimation of the mean response of ACF

Define a particular situation when the input of the ACF model is

$$f_0 = [f_1(z_{DG,1}^{(0)}) \quad \Lambda \quad f_1(z_{DG,m}^{(0)}) \quad f_2(z_{DG,1}^{(0)}) \quad \Lambda \quad f_2(z_{DG,m}^{(0)}) \quad f_3(z_{DG,1}^{(0)}) \quad \Lambda \quad f_3(z_{DG,m}^{(0)})].\mathrm{F}$$

or example, if considering the reciprocal of $|z_{DG,\lambda}|^3$ as the ACF model, the input matrix of the ACF model is,

$$f_0 = [|z_{DG,1}|^{-1} \quad \Lambda \quad |z_{DG,m}|^{-1} \quad |z_{DG,1}|^{-2} \quad \Lambda \quad |z_{DG,m}|^{-2} \quad |z_{DG,1}|^{-3} \quad \Lambda \quad |z_{DG,m}|^{-3}].$$

The ACF value can be estimated as $A\hat{C}F$ at a particular point by applying Equation (4.7f),

$$A\hat{C}F = \hat{y} = \sum_{\lambda=1}^{m} \hat{w}_{1,\lambda} \cdot |z_{DG,\lambda}|^{-1} + \sum_{\lambda=1}^{m} \hat{w}_{2,\lambda} \cdot |z_{DG,\lambda}|^{-2} + \sum_{\lambda=1}^{m} w_{3,\lambda} \cdot |z_{DG,\lambda}|^{-3}.$$

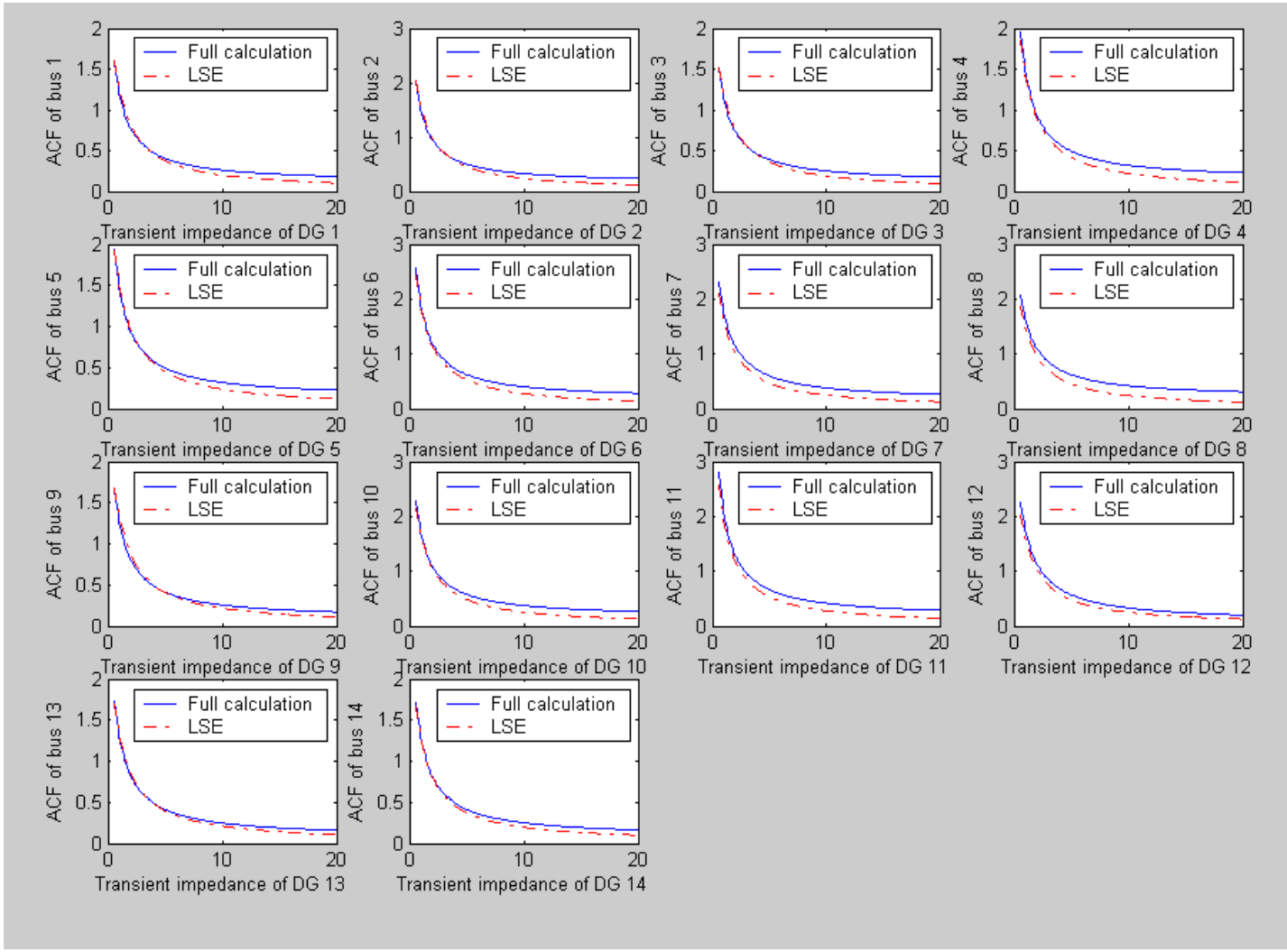

Figure 4.4 Comparison between the full fault calculation and the least squares estimator model, Case 4.1

Table 4.4 Confidence interval of the coefficient of the ACF model, Case 4.1

Model coefficient, $w_{j,\lambda}$	Ninety five percent Confidence interval	95% confidence interval / Coefficient $w_{j,\lambda}$
2.2048	± 0.2650	
2.5609	± 0.2433	0.1202
1.7878	± 0.2457	0.0950
2.3637	± 0.2564	0.1374
2.3148	± 0.2470	0.1085
2.7164	± 0.2310	0.1067
2.4916	± 0.2503	0.0850
2.3671	± 0.2548	0.1005
2.3834	± 0.2554	0.1076
2.6878	± 0.2830	0.1072
2.8195	± 0.2372	0.1053
2.8508	± 0.2695	0.0841
2.3576	± 0.2477	0.0945
2.2561	± 0.2572	0.1051
-1.1148	± 0.2195	0.1140
-1.2409	± 0.2001	0.1969
-0.8427	± 0.2009	0.1613
-1.1276	± 0.2126	0.2384
-1.1037	± 0.2021	0.1885
-1.1208	± 0.1879	0.1831
-1.1090	± 0.2057	0.1676
-1.1408	± 0.2113	0.1855
-1.2601	± 0.2104	0.1852
-1.2799	± 0.2342	0.1670
-1.1144	± 0.1945	0.1830
-1.4519	± 0.2254	0.1745
-1.2003	± 0.2052	0.1552
-1.1449	± 0.2126	0.1710
0.2317	± 0.0579	0.1857
0.2641	± 0.0523	0.2499
0.1711	± 0.0521	0.1980
0.2298	± 0.0559	0.3045
0.2259	± 0.0526	0.2433
0.2100	± 0.0485	0.2328
0.2113	± 0.0537	0.2310
0.2252	± 0.0556	0.2541
0.2692	± 0.0552	0.2469
0.2643	± 0.0617	0.2051
0.2006	± 0.0505	0.2334
0.2991	± 0.0601	0.2517
0.2523	± 0.0541	0.2009
0.2447	± 0.0559	0.2144
		0.2284

The variance of the $A\hat{C}F$ is

$$Var(A\hat{C}F) = \sigma^2 f_0'(F'F)^{-1} f_0 .$$

Therefore, 100(1-α) percent confidence interval on the mean response of the ACF model with f_0 as the input is [38],

$$A\hat{C}F_0 - t_{\alpha/2,n-p}\sqrt{\hat{\sigma}_r^{\,2} f_0'(F'F)^{-1} f_0} \le E(ACF|f_0) \le A\hat{C}F_0 + t_{\alpha/2,n-p}\sqrt{\hat{\sigma}_r^{\,2} f_0'(F'F)^{-1} f_0} . \tag{4.8}$$

For instance, the 95 percent confidence interval of ACF of the Thunderstone system with new DGs shown in Table 4.2 for Case 4.1 is,

$$10.63 - t_{0.025,467}\sqrt{\hat{\sigma}_r^{\,2} f_0'(F'F)^{-1} f_0} \le E(ACF|f_0) \le 10.63 + t_{0.025,467}\sqrt{\hat{\sigma}_r^{\,2} f_0'(F'F)^{-1} f_0} ,$$

or

$$10.53 \le E(ACF|f_0) \le 10.819 .$$

There is ninety five percent probability that the true ACF of Case 4.1 stays in the indicated interval. Table 4.5 shows the confidence interval of the mean response of the ACF model with various percent confidence, α.

Table 4.5 Percent confidence and their confidence intervals for the mean response of the ACF of the Thunderstone system, Case 4.1

Percent confidence	Confidence interval, $E(ACF\|f_0)$
98	10.63 ± 0.21
95	10.63 ± 0.18
90	10.63 ± 0.15
80	10.63 ± 0.12

4.6 Circuit breaker sizing

This section applies the *E/X* method with adjustment for AC and DC increments to choose the rated short-circuit current of CBs in the Thunderstone system according to IEEE/ANSI Standard C37.010 [30]. The single line diagram of the Thunderstone system is shown in Figure 3.1. The procedure for sizing the IC of CB is presented as the diagram in Figure 4.5. Table 4.6 shows the fault current calculations and *X/R* ratio for both three-phase and single line to ground bolted fault. After calculating *X/R* ratio of the system, the *X/R* multiplying factors for AC and DC increments are given in Figures 1.5 and 1.6.

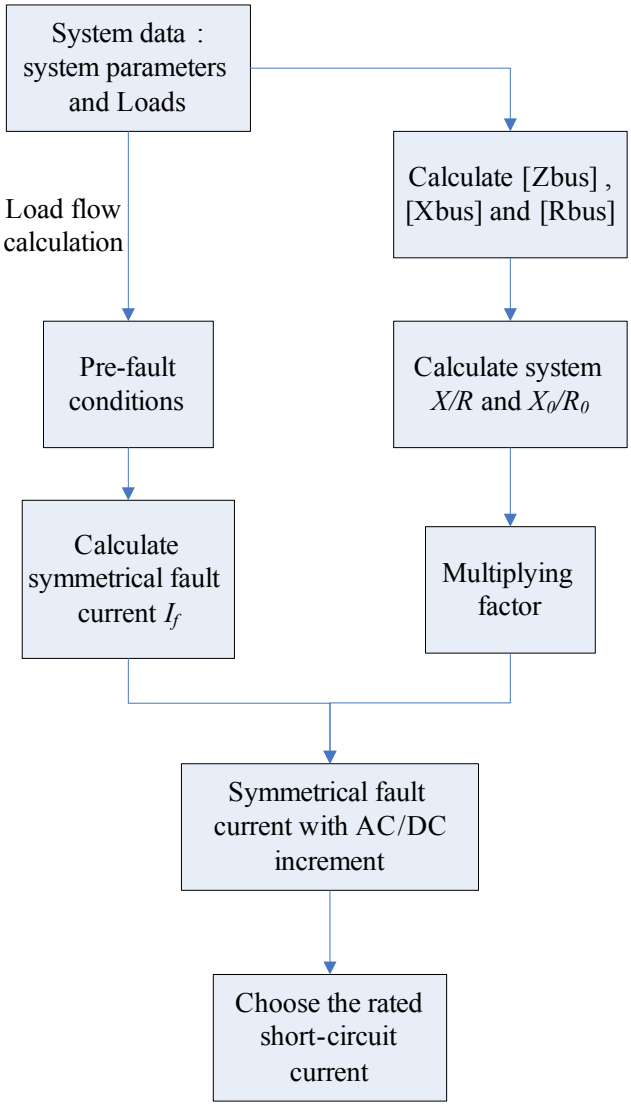

Figure 4.5 *E/X* method with adjustment for the AC and DC increment

Case 4.2 Application of the IEEE standard C37.04-1999 for sizing the CB

Assume that the locations of the bus with new DGs are shown in Table 4.2 and the positive and zero sequence transient impedance of the new DGs of every bus are 0.005+*j*1.0 p.u. and 0.0005+*j*0.7 p.u., respectively. According to the *E/X* ratio and multiplying factor, the IC of CB before installing DGs into the Thunderstone system can be chosen as shown in Table 4.7. The multiplying factor of CBs is chosen from 5-cycle CB with a contact parting time of 3 cycles. The preferred rating of CBs can be selected as provided in the ANSI standard C37.06-1997 [31]. Size of the CBs after installing DGs into the Thunderstone system is shown in Table 4.8.

Note that DGs are installed into the Thunderstone system at Cameron2, Signal13, Seaton2, Ealy3, Ealy4 and Sage. Evidently, the CBs at the bus with new DG should be upgraded due to the significant increase of fault currents. The cost of upgrading the CB at the local bus of DGs goes directly to the owner of DG. However, after installing the new DGs into the system, the fault current calculation shows that the IC of CBs at other location rather than only DG buses, such as Signal and Sage, also need to be upgraded. This indicates that not only the CBs of local bus of DGs should be upgraded, but also some 69-kV CBs in the area.

4.7 Allocation of the responsibility for the system upgrades to the owner of DGs

This section proposes a technique to allocate the responsibility of each DG owner due to the system upgrades by applying the ACF index. Theoretically, the owner of the DGs should share the cost for the system upgrades, depending on the severity of the change of fault created by their own DGs. According to the Thunderstone system, Case 4.2, six DGs are installed at the 12 kV bus. As the consequence of installing these DGs, the 69 kV CBs at 2 locations need to be upgraded. From Equation (4.6), the contributions of the DG at each bus are,

$$ACF_{(6)} = 2.5609 \cdot \frac{1}{\left|z_{DG,4}\right|} - 1.2409 \cdot \frac{1}{\left|z_{DG,4}\right|^2} + 0.2641 \cdot \frac{1}{\left|z_{DG,4}\right|^3} = 1.767\%,$$

$$ACF_{(11)} = 2.3148 \cdot \frac{1}{\left|z_{DG,11}\right|} - 1.1037 \cdot \frac{1}{\left|z_{DG,11}\right|^2} + 0.2259 \cdot \frac{1}{\left|z_{DG,11}\right|^3} = 1.610\%,$$

$$ACF_{(22)} = 2.6878 \cdot \frac{1}{\left|z_{DG,22}\right|} - 1.2799 \cdot \frac{1}{\left|z_{DG,22}\right|^2} + 0.2643 \cdot \frac{1}{\left|z_{DG,22}\right|^3} = 1.843\%,$$

$$ACF_{(24)} = 2.8195 \cdot \frac{1}{\left|z_{DG,24}\right|} - 1.1144 \cdot \frac{1}{\left|z_{DG,24}\right|^2} + 0.2006 \cdot \frac{1}{\left|z_{DG,24}\right|^3} = 2.101\%,$$

$$ACF_{(25)} = 2.8508 \cdot \frac{1}{\left|z_{DG,25}\right|} - 1.4519 \cdot \frac{1}{\left|z_{DG,25}\right|^2} + 0.2991 \cdot \frac{1}{\left|z_{DG,25}\right|^3} = 1.767\%,$$

$$ACF_{(26)} = 2.3576 \cdot \frac{1}{\left|z_{DG,26}\right|} - 1.2003 \cdot \frac{1}{\left|z_{DG,26}\right|^2} + 0.2523 \cdot \frac{1}{\left|z_{DG,26}\right|^3} = 1.531\%.$$

The owners of DG should pay for the cost of upgrading the protection system, such as IC of CBs and fuses, proportional to the ACF_i. For this reason, the cost for each owner of DG is distributed according to the following allocation,

$$\text{Price to the owner of DG at bus } \lambda = \frac{\text{Total cost for upgrades system}}{\sum_{\lambda}^{m} ACF_{(\lambda)}} \cdot ACF_{(\lambda)}, \quad (4.9)$$

where N is the number of the bus with DG.

Assuming that the cost of upgrading the CB at each of two locations is 50,000 dollars, the total upgrade cost in Equation (4.9) is 100,000 dollars. Then, the costs of upgrading the system for each owner of a DG are shown in Table 4.9.

In Equation (4.9), it is assumed that the entire CB upgrade costs should be assigned to the DG owners. If some fraction UF of the total cost is to be paid by the utility company, then 1-UF is paid by the DG owner,

$$\text{Price to the owner of DG at bus } i = (1 - UF) \cdot \frac{\text{Total cost for upgrades system}}{\sum_{\lambda}^{m} ACF_{(\lambda)}} \cdot ACF_{(\lambda)}.$$

Table 4.6 Fault current calculation for Thunderstone system, Case 4.2

Bus	Original System						System with new DGs					
	3-phase fault			SLG fault			3-phase fault			SLG fault		
	X/R	*E/X*	*E/Z*	*X/R*	*E/X*	*E/Z*	*X/R*	*E/X*	*E/Z*	*X/R*	*E/X*	*E/Z*
Thunder1	8.05	89.88	89.06	7.25	70.75	81.58	8.11	92.78	91.95	6.71	92.84	84.19
Thunder2	14.95	39.07	38.75	13.24	35.03	37.31	14.51	42.44	42.09	12.38	42.51	40.35
Cluff	10.24	25.50	25.25	6.89	9.55	16.15	10.04	27.49	27.22	4.51	27.53	17.44
Cluff2	3.08	1.59	1.52	3.10	1.46	1.48	3.07	1.61	1.54	3.01	1.61	1.50
Cameron	8.81	19.77	19.55	6.05	5.94	10.95	8.73	21.43	21.19	3.81	21.46	12.26
Cameron2	3.89	1.84	1.78	3.90	1.54	1.67	71.16	2.96	2.88	70.16	3.00	2.77
Noack	9.76	28.02	27.72	6.93	11.73	18.88	9.48	30.27	29.94	4.64	30.32	20.24
Noack2	2.99	1.51	1.45	3.00	1.42	1.43	2.99	1.53	1.47	2.94	1.53	1.45
Signal	7.96	23.95	23.60	6.00	9.24	15.36	7.80	26.48	26.09	4.21	26.53	17.57
Signal2	15.99	1.73	1.70	4.65	1.57	1.63	16.06	1.76	1.73	4.53	1.76	1.66
Signal3	3.01	1.57	1.50	3.03	1.43	1.45	76.90	2.70	2.59	75.84	2.74	2.55
Shanon	6.36	16.87	16.57	5.19	5.64	9.91	6.22	18.32	17.99	3.25	18.35	11.14
Shanon2	3.83	1.82	1.76	3.82	1.52	1.65	3.81	1.85	1.79	3.61	1.85	1.70
Superst	6.70	16.43	16.13	4.90	5.92	10.02	6.60	18.04	17.72	3.32	18.07	11.94
Superst4	3.55	1.35	1.30	3.52	1.19	1.25	3.53	1.38	1.33	3.40	1.38	1.29
Superst5	4.07	1.16	1.12	4.01	1.05	1.08	4.06	1.18	1.14	3.91	1.18	1.11

Table 4.6 (cont.) Fault current calculation for Thunderstone system, Case 4.2

Bus	Original System						System with new DGs					
	3-phase fault			SLG fault			3-phase fault			SLG fault		
	X/R	*E/X*	*E/Z*	*X/R*	*E/X*	*E/Z*	*X/R*	*E/X*	*E/Z*	*X/R*	*E/X*	*E/Z*
Sage	8.29	22.55	22.26	6.03	7.84	13.63	8.12	24.56	24.24	3.93	24.60	15.17
Sage2	1.80	1.55	1.37	1.84	1.38	1.33	1.79	1.57	1.39	1.76	1.57	1.35
McCoy	6.53	18.38	18.07	5.33	6.18	10.85	6.40	20.08	19.73	3.40	20.11	12.11
McCoy2	4.01	1.79	1.74	4.02	1.50	1.63	3.99	1.83	1.77	3.80	1.83	1.68
Seaton	6.49	19.25	18.92	5.21	6.97	11.85	6.48	21.60	21.22	3.75	21.64	13.96
Seaton2	3.08	1.53	1.46	3.10	1.36	1.40	77.49	2.68	2.57	76.40	2.72	2.52
Early	5.85	15.11	14.81	4.43	5.91	9.61	5.95	17.16	16.82	3.58	17.20	11.68
Early3	3.91	1.77	1.71	3.83	1.51	1.62	72.73	2.88	2.80	71.68	2.92	2.72
Early4	2.00	1.23	1.11	2.03	1.09	1.06	88.08	2.33	2.14	86.70	2.36	2.10
Sage3	3.29	1.54	1.48	3.31	1.38	1.42	78.79	2.65	2.55	77.66	2.68	2.50
Sage4	3.25	1.56	1.49	3.27	1.39	1.44	3.24	1.58	1.51	3.16	1.58	1.46

Table 4.7 Preferred ratings for CBs in Thunderstone system before installing DGs, Case 4.2

Bus	Rated continuous operating voltage kV, rms	*E/X* kA, rms	Multiplying Factor (3-cycle CB)	Rated short circuit current kA, rms
Thunder1	230	22.6	1.00	31.5
Thunder2	69	32.7	1.00	40
Cluff	69	21.3	1.00	31.5
Cluff2	12	7.7	1.00	12.5
Cameron	69	16.5	1.00	20
Cameron2	12	8.9	1.00	12.5
Noack	69	23.4	1.00	31.5
Noack2	12	7.3	1.00	12.5
Signal	69	19.7	1.00	20.0
Signal2	12	8.3	1.00	12.5
Signal3	12	7.6	1.00	12.5
Shanon	69	14.1	1.00	20
Shanon2	12	8.8	1.00	12.5
Superst	69	13.7	1.00	20
Superst4	12	6.5	1.00	12.5
Superst5	12	5.6	1.00	12.5
Sage	69	18.9	1.00	20
Sage2	12	7.5	1.00	12.5
McCoy	69	15.4	1.00	20
McCoy2	12	8.6	1.00	12.5
Seaton	69	16.1	1.00	20
Seaton2	12	7.4	1.00	12.5
Early	69	12.6	1.00	20
Early3	12	8.5	1.00	12.5
Early4	12	5.9	1.00	12.5
Sage3	12	7.4	1.00	12.5
Sage4	12	7.5	1.00	12.5

Table 4.8 Preferred ratings for CBs in Thunderstone system after installing DGs, Case 4.2

Bus	Rated continuous operating voltage kV, rms	E/X kA, rms	Multiplying Factor	Rated short circuit current kA, rms
Thunder1	230	23.3	1.00	31.5
Thunder2	69	35.6	1.00	40
Cluff	69	23.0	1.00	31.5
Cluff2	12	7.7	1.00	12.5
Cameron	69	18.0	1.00	20.0
Cameron2	12	14.4	1.30	20
Noack	69	25.4	1.00	31.5
Noack2	12	7.4	1.00	12.5
Signal	69	22.2	1.00	31.5
Signal2	12	8.5	1.00	12.5
Signal3	12	13.2	1.32	20
Shanon	69	15.4	1.00	20
Shanon2	12	8.9	1.00	12.5
Superst	69	15.1	1.00	20
Superst4	12	6.6	1.00	12.5
Superst5	12	5.7	1.00	12.5
Sage	69	20.6	1.08	31.5
Sage2	12	7.6	1.00	12.5
McCoy	69	16.8	1.02	20
McCoy2	12	8.8	1.00	12.5
Seaton	69	18.1	1.02	20
Seaton2	12	13.1	1.00	20
Early	69	14.4	1.01	20
Early3	12	14.0	1.00	20
Early4	12	11.4	1.00	20
Sage3	12	12.9	1.00	20
Sage4	12	7.6	1.00	12.5

Table 4.9 Cost for upgrades the system due to installing new DGs, Case 4.2

Bus name	Cost of upgrading the system, dollars
Cameron2 (6)	16,639.98
Signal3 (11)	15,161.50
Seaton2 (22)	17,355.68
Ealy3 (24)	19785.29
Ealy4 (25)	16,639.98
Sage3 (26)	14,417.55

4.8 Conclusions

The ACF of the Thunderstone system with the DGs in 6 locations, as shown in Figure 3.1, can be calculated by applying Equation (3.1). The results of ACF calculation are shown in Table 4.10.

The system model from the least squares method can be applied to calculate the ACF for the Thunderstone system. By applying the least squares method model, only the impedance of new DGs is required as an input to calculate the ACF.

One of the applications of the ACF index is to allocate the cost of upgrading the system. The cost of upgrades the system for each owner of DG mainly depends on the transient impedance of the DGs and the configuration of the system.

Even though the process of system design is done off-line, calculating an optimal power (OPF) is an online calculation. The least squares estimation of ACF may have an application in solving the OPF problem with fault current limitation.

For off line applications, such as in the process of system design, the exact calculation of the ACF (as discussed in Chapter 2 and 3) might be needed. However, the least squares estimation of the ACF index can be applied as a useful design tool for the customers with DG. Without providing the system parameters from the utility company, the customers with DGs can assess the severity of the increase of fault current from their DGs and the allocation of the cost of upgrades.

Table 4.10 The average change of fault current (ACF) due to installing new DG into the Thunderstone system, Case 4.1

New DG at Bus	Output of DG, MVA	Penetration Level (%)	ACF[1] (%)	Increment of ACF (%)	Maximum Change of Fault current[1] (%)	At bus[2]
6	25	9.2	1.73	1.73	3.85	5
6+11	25+19.1	16.4	3.43	1.70	5.01	5
6+11+22	25+19.1+20.2	24.1	5.39	1.96	6.82	21
6+11+22+24	25+19.1+20.2+20.0	31.7	7.66	2.27	9.98	23
6+11+22+24+25	25+19.1+20.2+20.0+7.9	34.8	9.43	1.77	14.02	23
6+11+22+24+25+26	25+19.1+20.2+20.0+7.9+15.1	40.6	10.87	1.44	15.08	23

Notes

1. Using conventional fault calculation
2. Consider only the bus without installing DG

5. Implication of Fault Current Increase on Optimal Power Flow

5.1 Implications of fault current in an OPF

There are several major objectives of calculating an OPF. One objective is to minimize the generation cost and calculate optimal setting for each generator in serving the load demand. Another objective is providing the information on economic analyses of the power system by determining the marginal cost data. In some application, the minimum fuel cost OPF is sufficient for obtaining power dispatch. The OPF can also include constraints that represent in the operation of the system, such as transmission capacity, voltage security and system stability. In this analysis, the fault current limitation is added as a constraint to the OPF. The ability of including different constraints and objective functions is sometimes needed in power system analysis. References [1, 35, 41] give an introduction to the OPF of electric power systems.

As discussed in Chapters 2 and 3, higher penetration levels due to installing DGs causes the increase of fault current. The increase of fault current may create problems during a fault, such as the potentially inappropriate setting of protection systems, nuisance trips and inadequate interruption capability of CBs. Fault current can be considered as a constraint in the OPF problem which may limit the operation of power systems. Many techniques can be applied to solve the OPF problem, such as the lambda iteration method, gradient methods, Newton's method, linear programming method (LPOPF) and the interior point method.

The example in this chapter introduces a totally preliminary study on the operating implications imposed by increased fault current due to the addition of DGs and/or merchant plans to a power system. The Thunderstone system (see Chapter 3 and Appendix A) is used to demonstrate a potential economic impact due to the high levels of DG and merchant plant penetration.

5.2 An illustration of operating implications of fault current

In this demonstration, four merchant plants are installed in the 69 kV bus of the Thunderstone system. This example is denominated as Case 5.1. In Case 5.1, operating limitations due to fault current are not included. In Case 5.2, the identical conditions to Case 5.1 are used except that fault current limit will be included. Table 5.1 shows the data of several merchant plants. These merchant plants are fictitious generating sources that are assumed to be available to operators of the Thunderstone system. Figure 5.1 shows the incremental fuel cost curves for the four merchant plants.

Table 5.1 Merchant plant data: Cases 5.1 and 5.2 (100 MVA base)

Location of merchant plant	Maximum capacity (MW)	Cost function ($/MWh)	$z_{DG,\lambda}$ (p.u.) *
Superstition (14)	50	$CF(P_1) = 20 + 0.4P_1$	$j0.1388$
Early (23)	20	$CF(P_1) = 20 + P_2$	$j0.69$
Signal (9)	10	$CF(P_1) = 20 + 2P_3$	$j0.69$
Cameron (5)	10	$CF(P_1) = 100 + 6P_4$	$j0.30$

The connection of these merchant plants to the Thunderstone system increases the fault current throughout the system. In some cases, especially when the system has high penetration level, the fault current after connecting these merchant plants may be higher than the interrupting capability of some CBs in the system. This means that the CBs may fail to interrupt fault current and may create a safety hazard.

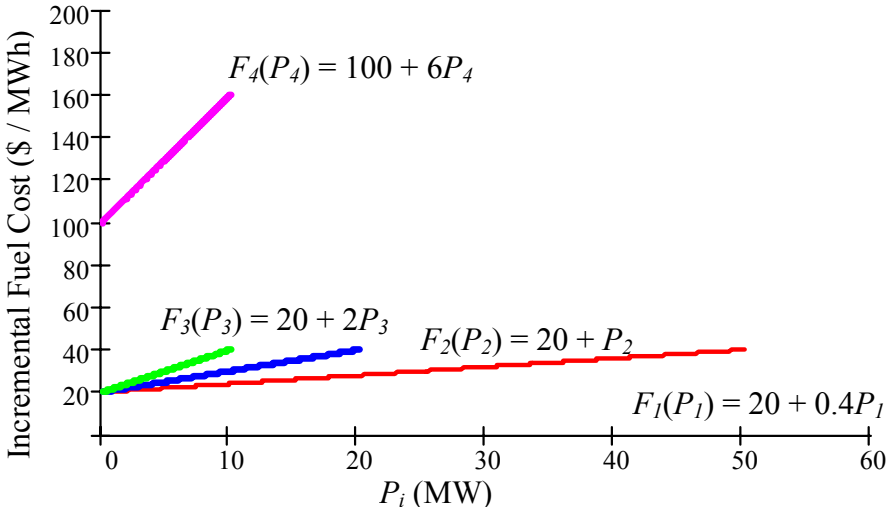

Figure 5.1 Incremental fuel cost of the merchant plants for Case 5.1 and 5.2

Assume that the interrupting capability of the CBs before connecting these merchant plants to the Thunderstone system is chosen as shown in Table 4.7 in Chapter 4. Example 5.1, four merchant plants are installed in the Thunderstone system. As shown in Table 5.2, there are 2^4 or 16 possible combinations of connecting these merchant plants. That is the operating status {off, off, off, off} to {on, on, on, on} represent 16 possible combinations. After analyzing the increase of fault current and resizing the CBs at each bus for all 16 cases by utilizing the technique discussed in Chapters 2 and 4, it is found that there are eight combinations such that some CBs in the system need to be upgraded. If the interrupting capability of the CBs is considered to be a constraint in the OPF problem, only seven combinations listed in Table 5.2 meet this constraint.

The following section compares the cost of generating at these merchant plants with and without the fault current limit as a constraint. For the ease of demonstration, the solution of this problem is done by the Equal Incremental Cost (EIC) technique and the results are shown in the following section.

Operational cost without fault current limitation: Case 5.1

Suppose these four merchant plants are requested to deliver a total power at 25 MW. The conditions for an optimum dispatch are,

$$20 + 0.4P_1 = \lambda$$
$$20 + P_2 = \lambda$$
$$20 + 2P_3 = \lambda$$

and

$$P_1 + P_2 + P_3 = 25.$$

In these equations, P_i is the generation at unit i in MW, and λ is the "system lambda" (i.e., the equal incremental cost of all cycling generation units [1, 35]). Solving the above equations,

$$\lambda = 26.25 \text{ \$/MWh}$$
$$P_1 = 15.625 \text{ MW}$$
$$P_2 = 6.25 \text{ MW}$$
$$P_3 = 3.125 \text{ MW}$$
$$P_4 = 0 \text{ MW}.$$

The optimum dispatch schedule for versus the total merchant plant generation is shown in Figure 5.2. The incremental cost is shown in Figure 5.3. The operating cost of generating a total of 25 MW is

$$\frac{1}{2}(26.25 + 20)(25) = 578.125 \text{ \$/h}$$

Note that the operating cost can be represented graphically by the shaded area in Figure 5.3.

Operational cost with fault current limitation: Case 5.2

According to Table 5.2, the fault current limit constraint forces the Units 1, 2 and 3 not to serve at the same time. In order to serve the demand within the constraint, the possible solutions are serving the load by only Unit 1 or by a combination of Units 2 and 3. The constrained case is denominated as Case 5.2

Suppose Unit 1 is set to serve the total demand of 25 MW, the conditions for optimal dispatch are,

$$20 + 0.4P_1 = \lambda$$

and

$$P_1 = 25 \text{ MW}.$$

The incremental cost, λ, is 30.0 \$/MWh and the operating cost is 625.0 \$/h.

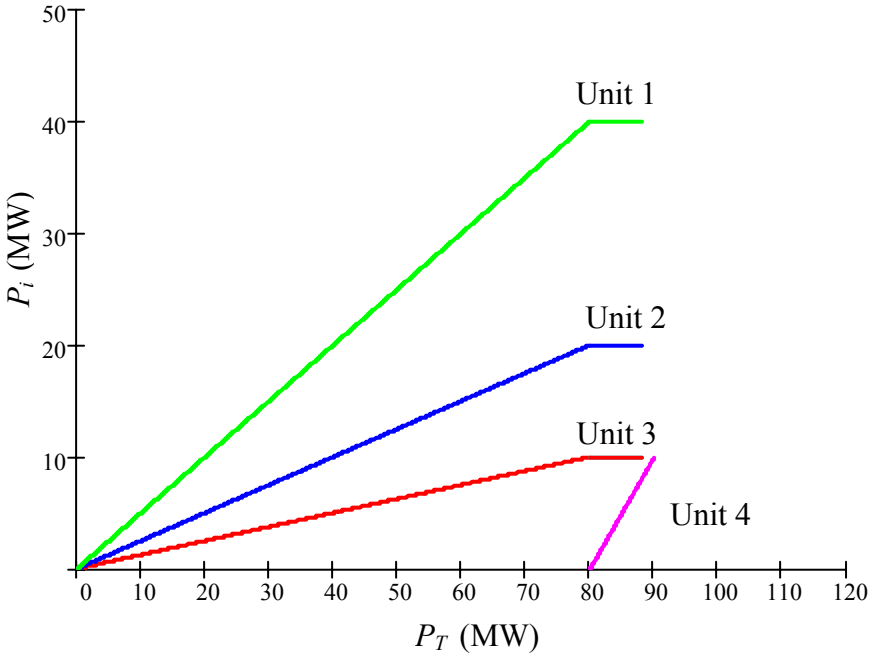

Figure 5.2 Economic dispatch for all units (without $|I_f|$ condition): Case 5.1

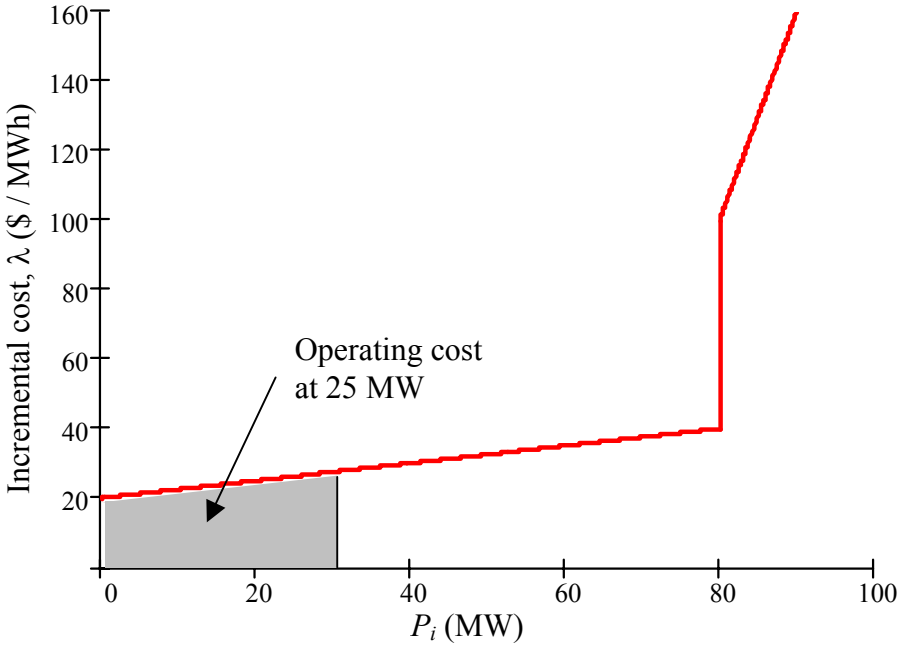

Figure 5.3 Incremental cost curve (without $|I_f|$ condition): Case 5.1

Suppose Units 2 and 3 are set to serve the total demand. The optimal conditions are,

$$20 + P_2 = \lambda$$
$$20 + 2P_3 = \lambda$$

and

$$P_2 + P_3 = 25 \text{ MW}.$$

Solving the equations,

$$\lambda = 36.67 \text{ \$/MWh}$$
$$P_2 = 16.67 \text{ MW}$$
$$P_3 = 8.33 \text{ MW}$$

and the incremental cost, λ, is 36.67 \$/MWh.

Table 5.2 Limitation of the system operation due to the increase of fault current, Case 5.2

Merchant plant locations (Connect □/ Disconnect X)				$\lvert I_f \rvert$ within CB limit
Superstition (14)	Cameron (5)	Signal (9)	Ealy (23)	
X	X	X	X	Y
X	X	X	□	Y
X	X	□	X	Y
X	X	□	□	Y
X	□	X	X	Y
X	□	X	□	Y
X	□	□	X	Y
X	□	□	□	N
□	X	X	X	Y
□	X	X	□	N
□	X	□	X	N
□	X	□	□	N
□	□	X	X	N
□	□	X	□	N
□	□	□	X	N
□	□	□	□	N

The cost of operation when Units 2 and 3 are in service is

$$\frac{1}{2}(36.667 + 20)25 = \ 708.33 \ \$/\text{h}.$$

The optimum schedule for Case 5.2 when Units 2 and 3 are in service and the incremental cost of operation are shown in Figures 5.4 and 5.5.

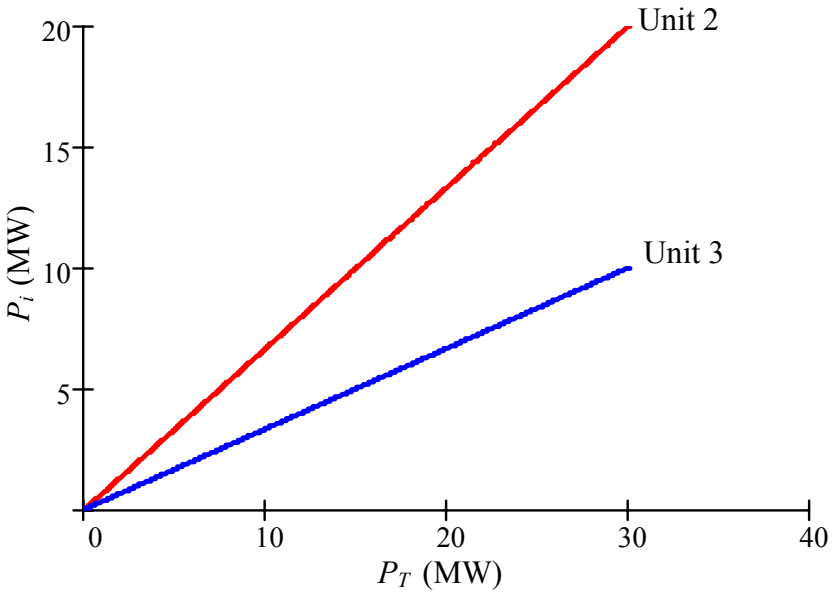

Figure 5.4 Economic dispatch for all units (with $|I_f|$ condition) when Unit 2 and 3 are in service, Case 5.2

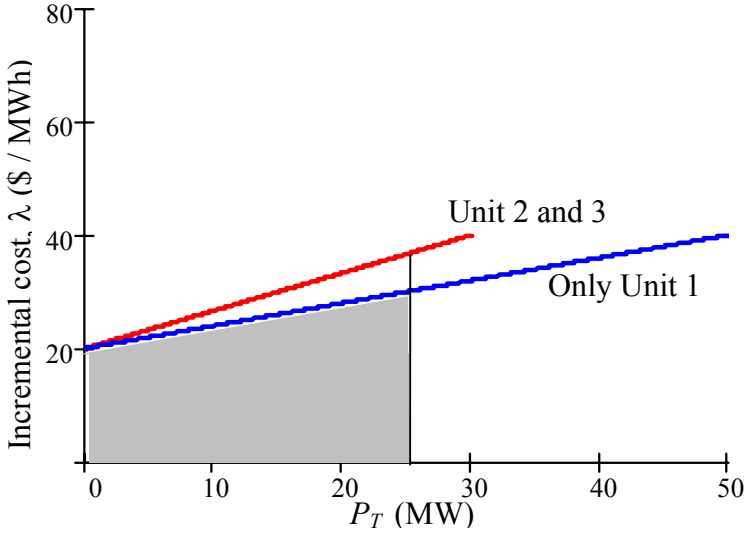

Figure 5.5 Incremental cost curve (with $|I_f|$ condition), Case 5.2

5.3 Production cost of the merchant plant under the fault current limitation constraint

The calculation of the constrained economic dispatch problem is shown in the previous section as Case 5.2. Note that serving the total demand of 25 MW by generations at Super, Cameron and Signal is the economic operating point when the fault current limit is neglected. However, serving the total demand by these three units does not meet the constraint. The constraint makes the system operator serve the demand only by using Unit 1. Table 5.3 shows the summary of the operating cost of merchant plants in Case 5.2.

Table 5.3 Operating cost of serving the demand: Case 5.2

Merchant plant locations (Connect / Disconnect X)				Operating cost of serving loads ($/h)		
Super (14)	Cameron (5)	Signal (9)	Ealy (23)	10 MW	25 MW	50 MW
X			X	233.3	708.3	-
	X	X	X	220.0	625.0	1,500.0
			X	212.5	578.1	1,312.5

5.4 Conclusions

New developments in deregulation have brought new generation sources, such as Independent Power Producers (IPPs) and DGs, to the system. IPPs and increased interconnection to utilize power from interchanges are new factors in fault current calculation. This chapter contains a preliminary illustration of the influence of fault current on the operating conditions of power systems. It demonstrated the potential economic impact arising from the increase of fault current due to the interconnection of new merchant plants. The case study shows that the generation of the merchant plants under the fault current limitation may result in higher cost of operation than the operation without this constraint.

6. Conclusions and Recommendations

6.1 Conclusions

Fault calculations in power systems are used to determine the interrupting capability of circuit breakers. The calculation of fault current at the system buses is done by applying the system Z_{bus} matrix. The effects of merchant plants, such as Independent Power Producers, are not taken into consideration in the classical fault current calculation. New developments in deregulation have brought new generation sources to the system. The appearance of DGs is a cause of increasing fault currents that has not previously been envisioned. This report presents a modification of the conventional fault current calculation in the case of addition of DGs.

Many consequences arise from increasing of the fault currents, for instance the change of coordination of protective devices, nuisance trips, safety degradation, and the requirement to change recloser and protective relay settings. These consequences result in the cost of equipment upgrades not only at the DG sites but also other system sites.

The equations for calculating the change of fault currents have been provided in Chapter 2 for the balanced three phase case. The Thunderstone system is used to illustrate the fault current calculation in Matlab. The results of the calculation are presented graphically in Chapter 3 and compared with the solutions from two power system analysis software packages: PowerWorld [33] and WinIGS [34].

Due to installing new DGs, six main factors that affect the severity of the increase of three phase fault current at each buses are:

- the number and size of DGs
- the operation of the AVR
- the impedance of DGs
- the location of DGs
- the type of DGs
- circuit breaker configuration.

Chapter 3 also proposes an index called the average change of fault current or "ACF". The ACF can be used to indicate the severity of the change of fault current due to installing new DGs. The application of ACF is illustrated in Case 3.3, 4.1 and 4.2. In order to calculate the exact solution of ACF, all system parameters, loads, pre-fault voltages and the calculation of fault currents of every bus are required. Chapter 4 proposes the least squares method to approximate the ACF for a given system. By this proposed technique, the pre-fault voltages and the fault current calculation may not be needed in the preliminary design stage. Note that in the preliminary design stage there may be a very large number of calculations, and the ACF concept can speed up the analysis. The only required input of the least squares method is the impedance of a new DG and its location. The advantages of this technique are:

- faster calculation due to the fact that load flow solution and fault calculations are not required
- contribution of the increase of fault current is indicated at each location of 12 kV bus in the primary distribution system. By this concept, each new DG is treated in an

equitable way. The ACF concept is offered as a rapid way to assess fault currents when DGs are deployed in any number, anywhere in the system.

The main disadvantage of the ACF method relates to accuracy. That is, even though the estimator may have been constructed for a large number of sample cases, there is no guarantee that the ACF calculation will be accurate.

The main subjects of this report and "claim of originality" are tabulated in Table 6.1.

Table 6.1 Summary of the topics in this report

Topic	Innovative concept	Classical concept
Fault current calculation		□
Increasing of fault current due to installing DGs	□	
Calculation of fault current with the present of DGs	□	□
CB sizing by E/X method with adjustment of AC and DC increments		□
Average Change of Fault (ACF) index	□	
Allocation of cost of upgrades	□	
Implication of fault current increase on OPF	□	

6.2 Potential new research areas

The following sections are the potential research areas related to power system fault current due to DGs:

The modeling of inverter based DGs

The study of fault current calculations in this report is done by assuming all DGs as synchronous generators. According to the demands for high reliability and power quality for sensitive loads, the demand for renewable generation sources is gradually rising. Renewable generation sources, such as fuel cells, microturbines, solar cells and wind turbines, are mostly based on electronic inverters. These inverter interfaces with the AC network result in changing of the fault response throughout the system. For this reason, the model of inverter based DGs should be included in this study. Included are transient models, single phase / three phase models, and models of the ultimate sources of the electrical energy (e.g. a fuel cell or a photovoltaic source).

Dollar cost of upgrading

For specific applications of DG, the cost of upgrading protection and interruption devices should be considered. And this dollar cost should be allocated properly. Minimizing the upgrade cost is one possibility. Sharing the cost is another alternative. The application of the ACF concept in this report is a further alternative. The economic is-

sues need to be analyzed in detail. The nonlinear relationship between $|I_f|$ and CB cost should be considered. Also, issues of the sequencing of DG installations should be considered. For example, if DGs are installed at A, B, and C and cost is allocated; then DGs are installed at D,E, and F, the final stage installation is different than if the installation sequence were {A, E, F}. Then {B, C, D} (for example).

Techniques for fault current reduction

Perhaps the solution to managing the rising of fault current lies in applying a technique to reduce the fault current. For example, fault current reduction is possible by installing a reactor in the system. There may also be solid state solutions to this problem. Each alternative needs to be studied in detail.

Security constrained OPF

There may be the circumstances in which a security constrained OPF needs to include constraints imposed by the IC of circuit breakers or the setting of protective relays. Distributed and alternative generation may impact these constraints. The impact of DG on OPF should be analyzed. Although this subject has been addressed in Chapter 5, it seems prudent that a much more detailed analysis of a constrained OPF should be done.

References

[1] G. T. Heydt, "Computer methods for power systems," Stars in a Circle Publications, Scottsdale, AZ, 1996.

[2] J. J. Grainger, W. D. Stevenson, "Power system analysis," McGraw-Hill, New York, 1994.

[3] G. W. Stagg, A. H. El-Abiad, "Computer methods in power systems analysis," McGraw-Hill, New York, 1994.

[4] P. M. Anderson, "Analysis of faulted power systems," IEEE PRESS Power System Engineering Series, New York, 1995.

[5] The US Department of Energy (DOE), Office of Distributed Energy Resources, www.eere.energy.gov/der/, 2003

[6] IEEE, "Standard for interconnecting distributed resources with electric power systems," IEEE Standard 1547-2003, 2003.

[7] H. B. Püttgen, P. R. Macgregor, F. C. Lambert, "Distributed generation semantic hype or the dawn of a new era," IEEE Power & Energy Magazine, vol. 1, pp. 22-29, Jan. / Feb. 2003.

[8] R. C. Dugan, T. E. McDermott, "Operating conflicts for distributed generation on distribution systems," Proceedings of the Rural Electric Power Conference, pp. A3/1-A3/6, 2001.

[9] Girgis, S. Brahma, "Effect of Distributed generation on protective device coordination in distribution system," Large Engineering Systems Conference (LESCOPE), Halifax NS, pp. 115-119, July 2001.

[10] J. G. Slootweg, W. L. Kling, "Impacts of distributed generation on power system transient stability," Power Engineering Society Summer Meeting, vol. 2, pp. 862-867, 2002.

[11] R. C. Dugan, "Issues for distributed generation in the US," Power Engineering Society Winter Meeting, vol. 1, pp. 121-126, Jan. 2002.

[12] R. C. Dugan, "On the necessity of three-phase feeder models for DG planning analysis," IEEE Power Engineering Society Summer Meeting, vol. 1, pp. 438-441, July 2002

[13] D. Candusso, L. Valero, A. Walter, "Modelling, control and simulation of a fuel cell based power supply system with energy management," IEEE Annual Conference of Industrial Electronics Society, vol. 2, pp. 1294-1299, Nov. 2002.

[14] C. J. Hatziadoniu, A. A. Lobo, F. Pourboghrat, M. Daneshdoost, **"**A simplified dynamic model of grid-connected fuel-cell generators," IEEE Transactions on Power Delivery, vol. 17, no. 2, pp. 467-473, Apr. 2002.

[15] T. Petru, T. Thiringer, "Modeling of wind turbines for power system studies," IEEE Transactions on Power Systems, vol. 17, no. 4, pp. 1132-1139, Nov. 2002.

[16] S. Jemeï, D. Hissei, M. C. Péra, J. M. Kauffmann, "Black-box modeling of proton exchange membrane fuel cell generators," IEEE Annual Conference 28th of Industrial Electronics Society, vol. 2, pp. 1474-1478, Nov. 2002.

[17] Y. Fukuyama, Y. Ueki, "Fault analysis system using neural networks and artificial intelligence," Proceedings of the Second International Forum on Applications of Neural Networks to Power Systems, pp. 20-25, Yokohama, Japan, Apr., 1993.

[18] F. B. Lazim, N. Hamzah, P. M. Arsad, "Application of ANN to power system fault analysis," Proceedings of Student Conference on Research and Development, pp. 269-273, Shah Alam, Malaysia, July, 2002.
[19] Distributed Coalition Power of America (DCPA), www.distributed-generation.com, 2002
[20] The Electric Power Research Institute (EPRI), http://www.epri.com/target.asp", 2002
[21] H. Zareipour, K. Bhattacharya, C. Canizares, "Distributed generation: current status and challenges," Proceedings of the IEEE North American Power Symposium (NAPS), pp. 392-399, Moscow, Idaho, 2004.
[22] Chambers, S. Hamilton, B. Schnoor, "Distributed generation: a nontechnical guide," PennWell Corporation, Tulsa, Oklahoma, 2001.
[23] T. Ackerman, G. Anderson, L. Soder, "Distributed generation: a definition," Electric Power System Research, vol. 57, pp. 195–204, 2001.
[24] "Impact of increasing contribution of dispersed generation on the power system," CIGRE study Committee no. 37, Final Report, 2003.
[25] J. Larminie, A. Dicks, "Fuel cell system explained," John Wiley & Sons, West Sussex, England, 2003.
[26] G. Hoogers, "Fuel cell technology handbook," CRC Press, Boca Raton, Florida, 2002.
[27] L. Castaner, S. Silvestre, "Modeling photovoltaic systems using PSpice," John Wiley & Sons, West Sussex, England, 2002.
[28] Arizona Public Service (APS), "Arizona PV cost," www.solarelectricpower.org, 2003
[29] IEEE, "Rating structure for AC high-voltage circuit breakers," IEEE Standard C37.04, 1999.
[30] IEEE, "Application guide for AC high-voltage circuit breakers rated on a symmetrical current basis," IEEE/ANSI Standard C37.010, 1999.
[31] ANSI, "AC high-voltage circuit breakers rated on a symmetrical current basis – preferred ratings and related required capabilities," ANSI Standard C37.06, 1997.
[32] N. Nimpitiwan, G. T. Heydt, "Fault current issues for market driven power systems with distributed generation," Proceedings of the North American Power Symposium (NAPS), pp. 400-406, Moscow, Idaho 2004.
[33] PowerWorld Corporation, www.powerworld.com, 2004.
[34] S. Meliopoulos, "WinIGS: integrated grounding system design program," Georgia Tech, March, 2004.
[35] Wood, B. Wollenberg, "Power generation operation and control," second edition, Wiley Interscience Publication, New York, 1996.
[36] ANSI, "Electric power systems and equipment - voltage ratings (60 Hz)," ANSI Standard C84.1, 1995.
[37] S. Haykin, "Neural networks: a comprehensive foundation," second edition, Prentice Hall, New York, 1999.
[38] D. Montgomery, E. Peck, G. Vining, "Introduction to linear regression analysis," third edition, Wiley Series in Probability and Statistics, New York, 2001.
[39] M. Huneault, F. D. Galiana, "A survey of the optimal power flow literature," IEEE Transactions on Power Systems, vol. 6, No. 2, pp. 762-770, May 1991.

[40] P. Venkataraman, “Applied optimization with Matlab programming,” Wiley Interscience, New York, 2001.
[41] M. E. El-Hawary, G. S. Christeiensen, “Optimal economic operation of electric power systems,” Academic Press, New York, 1987.
[42] D. Gan, R. J. Thomas, R. D. Zimmerman, “Stability-constrained optimal power flow,” IEEE Transactions on Power Systems, vol. 15, no. 2, pp. 535-539, May 2000.
[43] A. A. El-Keib, H. Ma, J. L. Hart, “Environmentally constrained economic dispatch using lagrangian relaxation method,” IEEE Transactions on Power Systems, vol. 9, no. 4, pp. 1723-1729, Nov. 1994.
[44] R. Ramanathan, “Emission constrained economic dispatch,” IEEE Transactions on Power Systems, vol. 9, no. 4, pp. 1994-2000, Nov. 1994.
[45] K. P. Wong, J. Yuryevich, “Evolutionary programming based algorithm for environmentally constrained economic dispatch,” IEEE Transactions on Power Systems, vol. 13, no. 2, pp. 301-306, May 1998.
[46] K. Deb, “Multi objective optimization using evolutionary algorithms,” Wiley Interscience series in systems and optimization, New York, 2001.
[47] T. Yalcinoz, H. Altun, “Environmentally constrained economic dispatch via a genetic algorithm with arithmetic crossover,” IEEE Africon, pp. 923-928, 2002.
[48] H. Ma, A. A. El-Keib, R. E. Smith, “A genetic algorithm based approach economic dispatch of power systems,” International Conference on Power Industry Computer Applications, pp. 207-212, May 2001.
[49] W. F. Tinney, J. M. Bright, K. D. Demaree, B. A. Hughes, “Some deficiencies in optimal power flow,” IEEE Transactions on Power Systems, vol. 3, no. 2, pp. 676-683, May 1988.
[50] K. C. Almeida, F. D. Galiana, “Critical cases in the optimal power flow,” IEEE Transactions on Power Systems, Vol. 11, no. 3, pp. 1509-1518, Aug. 1994.
[51] B. H. Chowdury, S. Rahman, “A review of recent advances in economic dispatch,” IEEE Transactions on Power Systems, vol. 5, no. 4, pp. 1248-1259, Nov. 1990.
[52] M. Huneault, F. D. Galiana, “A survey of the optimal power flow literature,” IEEE Transactions on Power Systems, vol. 6, no. 2, pp. 762-770, May 1991.
[53] Y. Jiang, S. Dongyuan, D. Xianzhong, T. Yuejin, C. Shijie, “Comparison of superconducting fault current limiter in power system,” Proceedings of Summer Meeting, Power Engineering Society, vol. 1, pp. 43-47, Jul. 2001.
[54] E. M. Lueng, “Superconducting fault current limiters,” IEEE Power Engineering Review, vol. 10, no. 8, pp. 15-18, Aug. 2000.
[55] A. J. Power, “An overview of transmission fault current limiters,” IEE Colloquium, pp. 1/1-1/5, Jun. 1995.
[56] X. Wu, J. Mutale, N. Jenkins, G. Strbac, “An investigation of network splitting for fault level reduction,” Technical report, Tyndal center of climate change research, Manchester Center for Electric Energy, Sep. 2003, http://www.tyndall.ac.uk/publications/working_papers/wp25.pdf.
[57] M. Sjöström, R. Cherkaoui and B. Dutoit, “Enhancement of power system transient stability using superconducting fault current limiters,” IEEE Transactions on Applied Superconductivity, vol. 9, no. 2, pp. 1328-1330, Jun. 1999.

[58] S. Lee, C. Lee, T. Ko, O. Kyun, "Stability analysis of a power system with superconducting fault current limiter installed," IEEE Transactions on Applied Superconductivity, vol. 11, no. 1, pp. 2098-2101, Mar. 2001.
[59] K. Hongesombut, Y. Mitani, K. Tsuji, "Optimal location assignment and design of superconducting fault current limiters applied to loop power systems," IEEE Transactions on Applied Superconductivity, vol. 13, no. 2, pp. 1828-1831, Jun. 2003.
[60] L. Ye, L. Lin, K. Juengst, "Application studies of superconducting fault current limiters in electric power system," IEEE Transactions on Applied Superconductivity, vol. 12, no. 1, pp. 900-903, Mar. 2002.
[61] E. Calixte, Y. Yokomizu, H. Shimizu, T. Matsumura, H. Fujita, "Reduction of rating required for circuit breakers by employing series connected fault current limiters," IEE Proceedings on Generation, Transmission and Distribution, vol. 151, no. 1, pp. 36-42, Jan. 2004.
[62] G. G. Karady, "Principles of fault current limitation by a resonant LC circuit," IEE Proceedings on Generation, Transmission and Distribution, vol. 139, no. 1, pp. 1-6, Jan. 1992.
[63] H. W. Dommel, W. F. Tinney, "Optimal Power Flow Solutions," IEEE Transactions on Power Apparatus and Systems, vol. PAS-87, pp. 1866-1867, Oct. 1968.

Appendix A

SYSTEM PARAMETERS OF THE THUNDERSTONE SYSTEM

This appendix shows the detail of system parameters of the Thunderstone system, such as line parameters, transformer impedance, loads and impedance of DGs. All parameters are used in the experiments in Chapter 3 and Chapter 4.

Table A.1 Transmission line parameter for Thunderstone system

69 kV Line			Per unit impedance @100°C (100 MVA Base)					
	FROM	TO	R1	X1	G1	B1	G2	B2
1	Cluff	Thundrst	0.00232	0.01552	0	0.0004		
2	Cluff	Cameron	0.00253	0.01636	0	0.00044	0	0.00046
3	Superst3	Cameron	0.01245	0.07996	0	0.00223	0	0.00223
4	Noak	Thundrst	0.00235	0.01295	0	0.00035	0	0.00034
5	Noak	SignalBu	0.00439	0.024	0	0.00064	0	0.00065
6	Shannon	SignalBu	0.00756	0.03097	0	0.00038	0	0.00038
7	Shannon	Superst4	0.00861	0.03572	0	0.00045	0	0.00045
8	SignalBu	Thundrst	0.01562	0.05749	0	0.00076		
9	Seaton	SignalBu	0.00868	0.03194	0	0.00042		
10	Sage	Thundrst	0.00436	0.02435	0	0.00064	0	0.00063
11	McCoy	Sage	0.00691	0.02809	0	0.00035		
12	McCoy	Seaton	0.00649	0.02638	0	0.00033		
13	Ealy	Seaton	0.00869	0.03517	0	0.00043	0	0.00043
14	Ealy	Superst1	0.01113	0.04134	0	0.00054		

Table A.2 Load bus data

Bus	MW	MVAR
Cluff	22	0.5
Cameron	27.1	0.5
Noack	21.6	0.8
SignalBU	43.8	2.1
Bay 3	22.3	0.3
Bay 4	21.5	1.8
Shanon	23.3	2.3
Superstition	39.6	3
Bay 2	16	3.2
Bay 3	23.6	0.2
Sage	56.4	6.5
Seaton	23.2	2.6
Ealy	30	2.4
Bay 2	21.4	0.4
Bay 4	8.6	2
McCoy	0	0

Table A.3 Substation transformer (230/69 kV) at Thunderstone substation

PU on a 100 MVA base		
R	*X*	*Bmag*
0.002	0.06	0
0.001	0.06	0
0.001	0.07	0
0.001	0.06	0

Table A.4 Distribution transformers

FROM	Bus kV	To	Bus kV	Rated MVA	p.u. at Rated MVA		*Bmag*
					R	*X*	
Cluff	69	Cluff LD1	12	12	0.024	0.0742	0
Cameron	69	Cameron LD1	12	15	0.02	0.078	0
Ealy LD1	69	Ealy LD2	12	15	0.0198	0.0779	0
Ealy LD2	69	Ealy LD4	12	10	0.0388	0.074	0
Mccoy	69	Mccoy LD2	12	15	0.0197	0.0758	0
Noack	69	Noack LD2	12	12	0.0232	0.076	0
Sage	69	Sage LD2	12	12.5	0.0422	0.0725	0
Sage	69	Sage LD3	12	12.5	0.0228	0.0744	0
Sage	69	Sage LD4	12	12.5	0.0228	0.0741	0
Seaton	69	Seaton LD1	12	12	0.0238	0.0733	0
Shanon	69	Shannon LD2	12	15	0.0198	0.0763	0
SignalBU	69	Signal LD3	12	12	0.037	0.069	0
SignalBU	69	Signal LD4	12	12	0.0243	0.073	0
Superstition	69	Superstition LD2	12	12	0.0233	0.083	0
Superstition	69	Superstition LD3	12	12	0.0239	0.1028	0

Appendix B

LIST OF CONDITIONS FOR ALL THE EXPERIMENTS

This appendix shows the summary of the experiment in this report. All experiments in Chapter 3 and Chapter 4 are simulated based on the Thunderstone system.

Table B.1 Summary of the case studies

Case	Locations of DG	Varied parameters	Target of experiments
3.1	Cameron2 Signal3 Sage3 Seaton2	Number and locations of DGs in the system	Severity of the change of fault current
3.2	Seaton Cameron2 Signal3 Sage3	AVR turn on/off	Severity of the change of fault current
3.3	Cameron2 Signal3 Sage3 Seaton2	Impedance of DGs	Severity of the change of fault current
4.1	Cameron2 Signal3 Seaton2 Ealy3 Ealy4 Sage3.	Impedance of DGs, location of new DGs	Illustrates application of the least squares estimator to calculate the ACF

Table B.1 Summary of the case studies (cont.)

Case	Locations of DG	Varied parameters	Target of experiments
4.2	Cameron2 Signal3 Seaton2 Ealy3 Ealy4 Sage3.	Impedance of DGs, location of new DGs	Shows the bus locations which need to be upgraded
5.1	Superstition (14) Early (23) Signal (9) Cameron (5)	Without considering the operating limitations	Operating implication imposed by the increase fault current
5.2	Superstition (14) Early (23) Signal (9) Cameron (5)	Consider the operating limitations	Operating implication imposed by the increase fault current